4-26-2004

Nondestructive Evaluation of Concrete Strength in the Precast Plant Using the Impact-Echo Method

Daniel Irwin

Stephen Pessiki

NONDESTRUCTIVE EVALUATION OF CONCRETE STRENGTH IN THE PRECAST PLANT USING THE IMPACT-ECHO METHOD

by

Daniel Irwin
dbi2@lehigh.edu

Stephen Pessiki
pessiki@lehigh.edu

ATLSS Report No. 04-10

April 26, 2004

ATLSS is a National Center for Engineering Research on Advanced Technology for Large Structural Systems

117 ATLSS Drive
Bethlehem, PA 18015-4728

Phone: (610)758-3525
Fax: (610)758-5902

www.atlss.lehigh.edu
Email: inatl@lehigh.edu

Mr. Daniel Irwin
Graduate Research Assistant

Dr. Stephen Pessiki
Professor of Structural Engineering

ACKNOWLEDGEMENTS

This report is based upon research supported by a 2002 Daniel P. Jenny Fellowship granted by the Precast/Prestressed Concrete Institute. Additional support was provided by High Concrete Structures, Inc., Metromont Prestress Company, Tindall Corporation, and the Pennsylvania Infrastructure Technology Alliance. The findings and opinions expressed in this report are those of the authors.

TABLE OF CONTENTS

ABSTRACT

Concrete compressive strength is a key parameter controlling the production of precast concrete members. In current practice, concrete compressive strength is often determined by compression tests of cylinders made from the same concrete as the concrete members. The cylinders are cured in a manner that is intended to replicate the curing conditions in the concrete members.

In the impact-echo method, a stress pulse is introduced into an object by a mechanical impact on its surface. This pulse undergoes multiple reflections, or echoes, between opposite faces of the object. The reflected pulse creates a surface displacement which is monitored adjacent to the point of impact, and the frequency of pulse arrivals is determined. The thickness of the object is known and is used along with the frequency of the pulse arrivals to determine the compression (P-wave) velocity.

Previous research demonstrated that the impact-echo method can be used to estimate the compressive strength of a concrete cylinder using the relationship between compressive strength and velocity. The objective of the research presented in this report is to explore the use of the impact-echo method to evaluate the early-age mechanical properties of concrete in a precast plant. Two specific applications are evaluated: (1) use of the impact-echo method as a tool for quality control of concrete mixtures in a precast plant; and (2) use of the impact-echo method to predict the time when a particular concrete compressive strength will be reached.

Two concrete mixtures were tested with one acting as a control and the other as a variant. The strength-velocity relationship of the control mixture was statistically compared with that of the variant and the observed differences were used to establish guidelines for quality control. Confidence limits were calculated for the log of strength versus velocity data from the experiments utilizing the control mixture. When data from the variant mixture was superimposed on the limits, it crossed outside of the limits. Therefore, confidence limits can be used with the impact-echo method to monitor deviations in the ingredients of a concrete mixture.

The control mixture was tested several times with different set-controlling admixtures, producing varying set times and rates of strength gain. This data was examined and a procedure to evaluate the rate of strength gain was developed. Examination of the experimental data revealed that the log of strength versus age relationship of a concrete mixture is approximately bi-linear. A general method, using this relationship, is proposed to predict the time when a concrete mixture reaches a target compressive strength.

CHAPTER 1

INTRODUCTION

1.1 INTRODUCTION

Concrete compressive strength is a key parameter used to control the production of precast concrete members. For example, operations such as termination of steam curing and transfer of prestress may be controlled by the compressive strength of the concrete. In current practice, concrete compressive strength is often determined by compression tests of cylinders made from the same concrete as the concrete members. The cylinders are cured in a manner that is intended to replicate the curing conditions in the actual concrete members.

In the impact-echo method, a stress pulse is introduced into an object by a mechanical impact on its surface. This pulse undergoes multiple reflections, or echoes, between opposite faces of the object. The reflected pulse creates a surface displacement which is monitored adjacent to the point of impact, and the frequency of pulse arrivals is determined. The thickness of the object is known and is used along with the frequency of the pulse arrivals to determine the compression (P-wave) velocity. Strength is nondestructively estimated from a previously established correlation between concrete strength and P-wave velocity.

1.2 OBJECTIVE

Previous research has demonstrated that the impact-echo method can be used to estimate the compressive strength of a concrete cylinder. The objective of the research presented in this report is to explore the use of the impact-echo method to evaluate the early-age mechanical properties of concrete in a precast plant. Two specific potential applications will be evaluated: (1) use of the impact-echo method as a tool for quality control of concrete mixtures in a precast plant; and (2) use of the impact-echo method as a means to predict the time when a particular concrete compressive strength (e.g. the transfer strength) will be reached.

1.3 SUMMARY OF APPROACH

1.3.1 General Description of Procedure Used in All Experiments

Tests were performed on seven batches of concrete cylinders in a precast plant. Six of the seven batches of cylinders were made with the same concrete mixture, and the other batch utilized a different concrete mixture. The cylinders were 152mm diameter by 305mm high (6 inch x 12 inch) in size and were prepared in accordance with ASTM standards. The impact-echo method was used to measure the P-wave velocity and this

data was recorded along with the time of the test. Immediately following the impact-echo test, the cylinder was tested in compression and the compressive strength was recorded. This procedure was repeated many times in order to gather an adequate amount of data to meet the research goals.

1.3.2 Using the Impact-Echo Method as a Tool for Quality Control

As noted above, most of the experiments tested the same concrete mixture; however, a second concrete mixture with different ingredients was also tested. The estimated strength-velocity relationship of this second concrete mixture was statistically compared with the estimated strength-velocity relationship from the other concrete mixture and the observed differences were used to establish guidelines for quality control of a concrete mixture based upon P-wave velocity and estimated strength.

1.3.3 Evaluating Rate of Strength Gain

As stated in Section 1.3.2, most of the experiments tested the same concrete mixture. This concrete mixture was tested during different times of the year and with different set-controlling admixtures, which produced varying set times and rates of strength gain. This data was examined and a procedure to evaluate the rate of strength gain was developed based on the data collected.

1.4 SCOPE OF REPORT

Chapter 2 presents background information necessary to understand the concepts presented in this report. This includes an in-depth discussion of the impact-echo method, a procedure for fitting a curve to strength-velocity data, and an explanation of the statistical methods used in the research.

Chapter 3 discusses the experimental program utilized to investigate the research goals. This includes a description of the test matrix, a description of specimen preparation and handling, and a description of the specimen testing procedure.

Chapter 4 discusses the results from a typical experiment. The pertinent plots used to examine the data from impact-echo testing are shown along with a discussion of important characteristics of each of the plots.

Chapter 5 presents the results of examining the possible use of the impact-echo method as a tool for quality control. A specific example for calculating a confidence limit is given, followed by the results of using a confidence limit to identify a concrete mixture with a different strength-velocity relationship. Lastly, a suggested list of guidelines for using the impact-echo method as a tool for quality control is given.

Chapter 6 presents the results of using the impact-echo method to predict time to reach a target strength by measuring the rate of strength gain of concrete. The general approach

to predict time of a target strength is given, followed by three variations of this approach that were used. Lastly, the three variations are compared and the preferred method is identified.

Chapter 7 contains a summary of the report, as well as a summary of the conclusions from Chapters 5 and 6.

1.5 NOTATION

The following is a description of the notation used in this report.

C - wave velocity (general notation)
C_p - P-wave velocity
E - elastic modulus
f_c - concrete compressive strength
$f_{c,\,target}$ – target strength of a concrete mixture
f_p - frequency of P-wave arrivals
n - number of degrees of freedom (number of points)
n_c - number of data points captured
s - sampling interval
S_{xx} - statistical calculation (see Chapter 2 for specific definition)
T - thickness of specimen
$t_{\alpha/2,n-2}$ - t-distribution multiplier
$\bar{x}$ - mean of the x-values
x_o - x-coordinate of regression line
Z - acoustic impedance
Δf - frequency resolution
Δt - time interval between P-wave arrivals
$\mu_{Y|xo}$ - y-coordinate of regression line
υ - Poisson's ratio
ρ - material density
σ^2 - standard error

CHAPTER 2

BACKGROUND

2.1 INTRODUCTION

This chapter presents the background information which is necessary to understand the concepts presented in the report. First, a review of relevant research involving the impact-echo method is given. Following this is an in-depth description of the impact-echo method. Next, a procedure for fitting a curve to a strength-velocity relationship is given. Finally, background information explaining the statistical methods which were used in the research is presented.

2.2 PREVIOUS APPLICATIONS OF THE IMPACT-ECHO METHOD TO EARLY AGE CONCRETE

Pessiki and Carino (1988) used the impact-echo method to study strength gain of concrete. The use of the method as a means of strength estimation was evaluated by exploring the relationship between concrete strength and P-wave velocity measured using the impact-echo method. This early work involved tests performed on 102mm x 203mm (4 inch x 8 inch) concrete cylinders. Pessiki and Carino concluded that the use of a strength-velocity relationship may be a useful approach for estimating concrete strength at early maturity. Successful impact-echo tests can be made at very early ages when the concrete has low compressive strength, in the range of 0.34 MPa (50 psi). Pessiki and Carino also concluded that the use of the impact-echo method to nondestructively estimate the in-place strength of concrete should be limited to the estimation of early-age strength. This is because the P-wave velocity is more sensitive to concrete strength at a low strength (early age) than at high strength. This is shown later in the chapter. The results by Pessiki and Carino also demonstrated the importance of concrete mixture uniformity. Careful control must be exercised over concrete mixture proportions, specifically the volume fraction of aggregate, for an empirical strength-velocity relationship to be used to estimate concrete strength.

Pessiki and Johnson (1996) used the impact-echo method to estimate early-age concrete strength in plate-like elements such as slabs and walls to explore whether it is possible to measure P-wave velocity in a large volume of concrete. They found that it is feasible to use the impact-echo method for these purposes. They also found, as expected, that strength-velocity plots from prepared cylinders and cores are not directly applicable to plate-like structures. This is due in part to the difference in P-wave velocity in plates (slabs, walls) versus rods (cylinders, cores) made out of the same material. Finally, they found that successful impact-echo tests to determine P-wave velocity can be made while the concrete has very low strength. Specifically, it was found that successful impact-echo

tests could be made about 3 hours before the first cores could be removed from a slab at a core compressive strength of about 4.48 MPa (650 psi).

Pessiki and Rowe (1997) investigated the influence of the presence of embedded steel reinforcing bars on the ability to measure P-wave velocity in early-age concrete. They found that the presence of reinforcing bars did not prevent successful measurement of P-wave velocity in early-age concrete.

2.3 DETAILED EXPLANATION OF THE IMPACT-ECHO METHOD

2.3.1 Stress Waves Caused by an Impact

Three types of stress waves are generated by an impact on the surface of an elastic solid: a surface (R) wave, a distortional (S) wave, and a dilatational (P) wave. The wavefronts caused by a point impact are shown in Figure 2.1.

The R-wave, or Raleigh Wave propagates along the surface in a circular pattern whereas the S and P-waves propagate from the impact point into the solid along hemispherical shaped wavefronts. The P-wave is associated with normal stress and the S-wave is associated with shearing stress. The impact-echo method is based upon monitoring the surface displacements caused by propagation of the P-wave, which will be the focus of the remainder of the information presented in this section.

The velocity of a P-wave propagating through an infinite elastic medium is dependent upon the elastic modulus of the material, E, the material density, ρ, and Poisson's ratio, υ. P-wave velocity can vary depending on the dimensions of the solid relative to the wavelength of the propagating wave. In an infinite elastic solid, the P-wave velocity, C_p, is given by Equation 2.1

$$C_p = \left[\frac{E(1-\nu)}{(1+\nu)(1-2\nu)\rho} \right]^{1/2} \qquad (2.1)$$

For rod-like structures free to expand laterally, the stress component perpendicular to the axis of the rod becomes negligible and the P-wave velocity approaches what is termed the longitudinal rod velocity, or

$$C_p = \left[\frac{E}{\rho} \right]^{1/2} \qquad (2.2)$$

2.3.2 Reflection and Transmission of Stress Waves at an Interface

The acoustic impedance, Z, of a material is equal to the product of the density of the material, ρ, and the wave speed, C, in the material or

$$Z = \rho C \qquad (2.3)$$

An acoustic interface is the interface or boundary between two materials with differing acoustic impedances. When a stress wave encounters this interface, reflection and transmission occurs. This reflection and transmission is dependent upon the angle of incidence and the acoustic impedance of each material.

The research presented in this report involves an acoustic interface between concrete and air, with concrete having a much higher acoustic impedance than air. In this case, the stress waves for a P-wave caused by an impact on the surface are shown in Figure 2.2, which is showing a single ray along the wavefront, offset laterally after each reflection for clarity.

The initial stress wave propagates downward in the form of a compression wave and is represented by a solid line. When the wave reaches the acoustic interface between the concrete and air, the sign of the wave changes and it is reflected back towards the surface as a tension wave. The tension wave is represented by a dashed line. When the tension wave returns to the top surface, which is also a concrete-air interface, the sign changes again and it is reflected back downward as a compression wave. These reflections and sign changes continue until the wave eventually damps out.

2.3.3 Determination of P-Wave Velocity

As stated in Section 2.3.2, the P-wave undergoes multiple reflections between the top and bottom surfaces of the specimen until damped out. Each arrival of the P-wave at the point of impact causes a surface displacement. The time-history of the surface displacement, or displacement waveform, is obtained with a displacement transducer positioned adjacent to the point of impact. An idealized displacement waveform is depicted in Figure 2.3.

The P-wave arrivals at the surface are noted in the figure by the nomenclature of 2P, 4P, and 6P. In this nomenclature 2P denotes a wave that has traveled twice the thickness of the test object (i.e. down and back). Similarly, 4P denotes a wave that has traveled four times the thickness of the test object (i.e. down and back twice). The time interval between each of these arrivals is called Δt. The path length traveled by the P-wave between each successive arrival at the top surface is two times the thickness of the specimen, or 2T. Therefore, the P-wave velocity can be calculated by the formula

$$C_P = \frac{2T}{\Delta t} \qquad (2.4)$$

The P-wave arrivals are not always clear in the actual displacement waveform and thus the waveform is transformed into the frequency domain using a Fourier transform. This transformation allows the periodicity of the P-wave reflections to be easily found. An idealized plot of a displacement waveform transformed into the frequency domain is shown in Figure 2.4.

The dominant peak in the frequency spectrum is the frequency of the P-wave arrivals, or f_p. The time interval between successive arrivals at the surface of the specimen is the inverse of the frequency of the P-wave, or

$$\Delta t = \frac{1}{f_P} \tag{2.5}$$

Therefore Equation 2.4 becomes

$$C_P = 2Tf_P \tag{2.6}$$

In this report the impact-echo tests are interpreted using the frequency domain and C_p is calculated using Equation 2.6.

2.3.4 Resolution in the Frequency Domain

The accuracy of the measurements in the frequency domain is governed by the number of points captured and the sampling interval. This is known as frequency resolution, or Δf. The formula to calculate the frequency resolution is

$$\Delta f = \frac{1}{n_c s} \tag{2.7}$$

where n_c is the number of points captured and s is the sampling interval. The equipment utilized in the experiments captured 1000 points in each displacement waveform. The sampling interval was varied from 2μs to 5μs and ultimately to 10μs as the concrete cured. The variation was due to the fact that P-waves damp out quickly when the concrete is at early age. Longer sampling intervals tended to lower the amplitude peak of the P-wave in the frequency domain because part of the record would contain no data since the P-wave had damped out. This makes the frequency of arrival of the P-wave more difficult to discern. As the concrete cures, the sampling interval can be increased, which, according to Equation 2.7, gives better resolution in the frequency domain. The resolution for the three sampling intervals used in the research is calculated as

$$2\mu s: \ \Delta f = \frac{1}{(1000)(0.000002)} = \pm 500Hz$$

$$5\mu s: \ \Delta f = \frac{1}{(1000)(0.000005)} = \pm 200Hz$$

$$10\mu s: \ \Delta f = \frac{1}{(1000)(0.000010)} = \pm 100Hz$$

Using these resolution values and Equation 2.6, the corresponding values for P-wave velocity resolution can be calculated for the 305mm thick concrete cylinders tested:

$$2\mu s: \ C_P = \frac{(2)(305mm)(500Hz)}{1000^2} = \pm 0.305km/s$$

$$5\mu s: \ C_P = \frac{(2)(305mm)(200Hz)}{1000^2} = \pm 0.122km/s$$

$$10\mu s: \ C_P = \frac{(2)(305mm)(100Hz)}{1000^2} = \pm 0.061km/s$$

2.4 FITTING A CURVE TO THE STRENGTH-VELOCITY DATA

Pessiki and Johnson (1996) developed a method to fit a curve to the strength-velocity data. That method is briefly described here. Figure 2.5 shows a typical set of strength-velocity data from the current research, which is described in Chapter 3.

An exponential model was found to fit the strength-velocity data and is of the form

$$f_C = ae^{C_P b} \qquad (2.8)$$

The compressive strength of the concrete is f_c, and a and b are constants. It was found that transforming the strength-velocity plot into semi-log space linearized the data and the resulting transformation of Equation 2.8 is thus

$$\ln(f_C) = \ln(a) + bC_P \qquad (2.9a)$$

Equation 2.9a is in the form of the equation of a straight line,

$$y = b + mx \qquad (2.9b)$$

A linear regression analysis can be performed on the data with C_p as the independent variable and f_c as the dependent variable. The values of a and b in Equation 2.9a are the intercept and slope, respectively, of the regression line. Figure 2.6 shows a plot of the natural log of strength versus velocity. The data in Figure 2.5 was used to produce this plot.

There is one final point to make using Figure 2.5. As stated earlier, Pessiki and Carino (1988) concluded that the impact-echo method is a more useful way to estimate concrete strength at earlier ages as compared to later ages. This is because, as shown in Figure 2.5, the velocity is changing rapidly relative to strength at early ages. Thus, even small increases in strength will be revealed by relatively large changes in velocity. At later ages, the opposite is true. Relatively large changes in strength may occur, but only small changes in velocity will occur to indicate this strength change. Thus, the method is more sensitive at earlier ages.

2.5 STATISTICAL ANALYSIS OF IMPACT-ECHO RESULTS

2.5.1 Introduction

This section explains how statistical analysis can be applied to the strength-velocity data to determine if two sets of data are from the same concrete mixture or from two different concrete mixtures. This is done with a view towards using the impact-echo method as a tool for quality control. For example, unintended variations in concrete mixture proportions or unintended variations the quality of concrete mixture ingredients may cause a change in the strength-velocity relationship. If statistical analysis can be used to detect this change, then it can alert production personnel about possible changes in the performance of the concrete due to these unintended effects. The use of statistical analysis of impact-echo results and quality control are treated in Chapter 5.

2.5.2 Confidence Limits

One of the simplest methods of applying a statistical test to the data from the impact-echo method is by using a 2-sided confidence limit on the mean, where the mean is the regression line that is fitted to the data using the methods in Section 2.4. The confidence limit calculates upper and lower bounds on the regression line based on a chosen percentage parameter for accuracy, which was 95% in the experiments performed in this research.

Figure 2.7 shows a plot of the upper and lower limits on the regression line from Figure 2.6. According to Montgomery and Runger (1994), the confidence limits are calculated using Equation 2.10

$$\mu_{Y|x_o} \pm t_{\alpha/2,n-2}\sqrt{\sigma^2\left[\frac{1}{n} + \frac{\left(x_o - \bar{x}\right)^2}{S_{xx}}\right]} \qquad (2.10)$$

where $\mu_{Y|x_o}$ is the y-coordinate calculated from the equation of the regression line at the coordinate x_o. $t_{\alpha/2,n-2}$ is a multiplier from the t-distribution, which is a point-estimation function where α/2 is defined as one half of the difference between 1 and the chosen confidence limit, which in this case is 0.95, and n-2 is the number of degrees of freedom less 2. σ^2 is defined as the standard error, and n is the number of degrees of freedom. $\left(x_o - \bar{x}\right)^2$ is the square of the difference between the current x-coordinate, x_o, and the mean. Finally S_{xx} is the sum of the squares of the x-values minus the sum of the x-values squared divided by the number of points or

$$\sum_{i=1}^{n} x_i^2 - \frac{\left(\sum_{i=1}^{n} x_i\right)^2}{n} \qquad (2.11)$$

The upper 95% limit is calculated with the positive value of the second term listed in Equation 2.10, whereas the lower 95% limit is calculated using the negative value. If calculations are made using several different x_o values, confidence limits for the entire regression line can be calculated and plotted as shown in Figure 2.7.

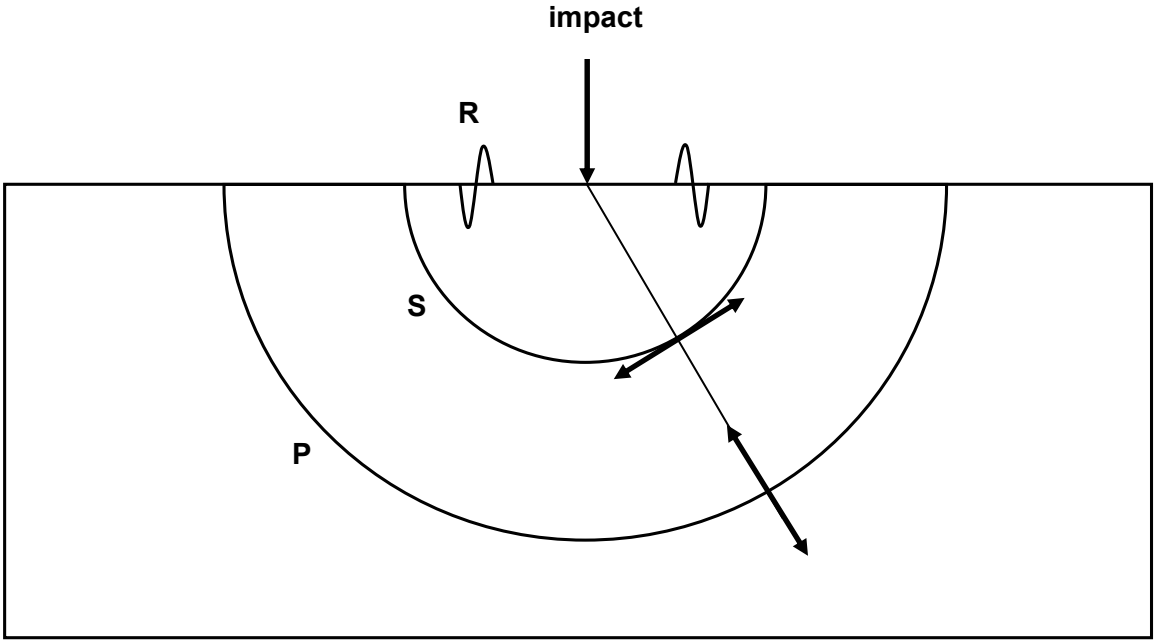

Figure 2.1 – Wavefronts of P, S, and R-waves caused by a point impact on the surface of an object

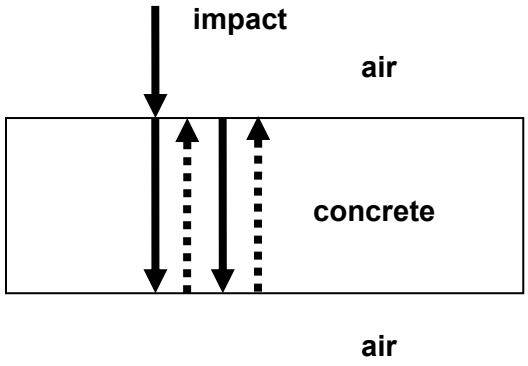

Figure 2.2 – Reflections of P-waves in experimental specimens

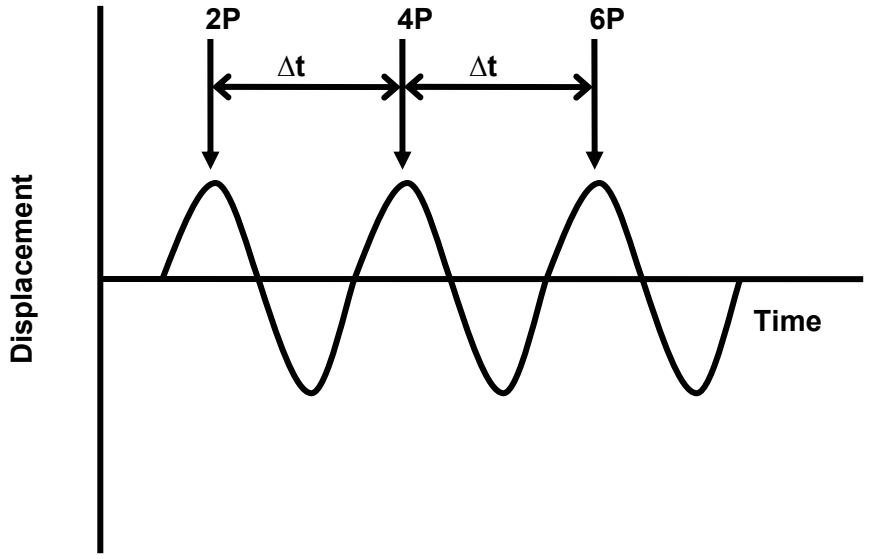

Figure 2.3 – Displacement versus time waveform

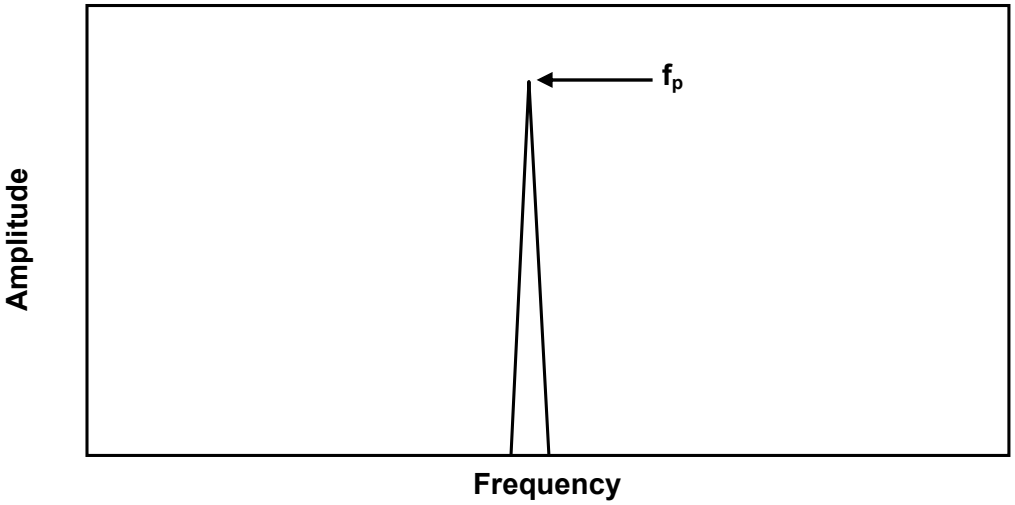

Figure 2.4 – Plot of the frequency domain

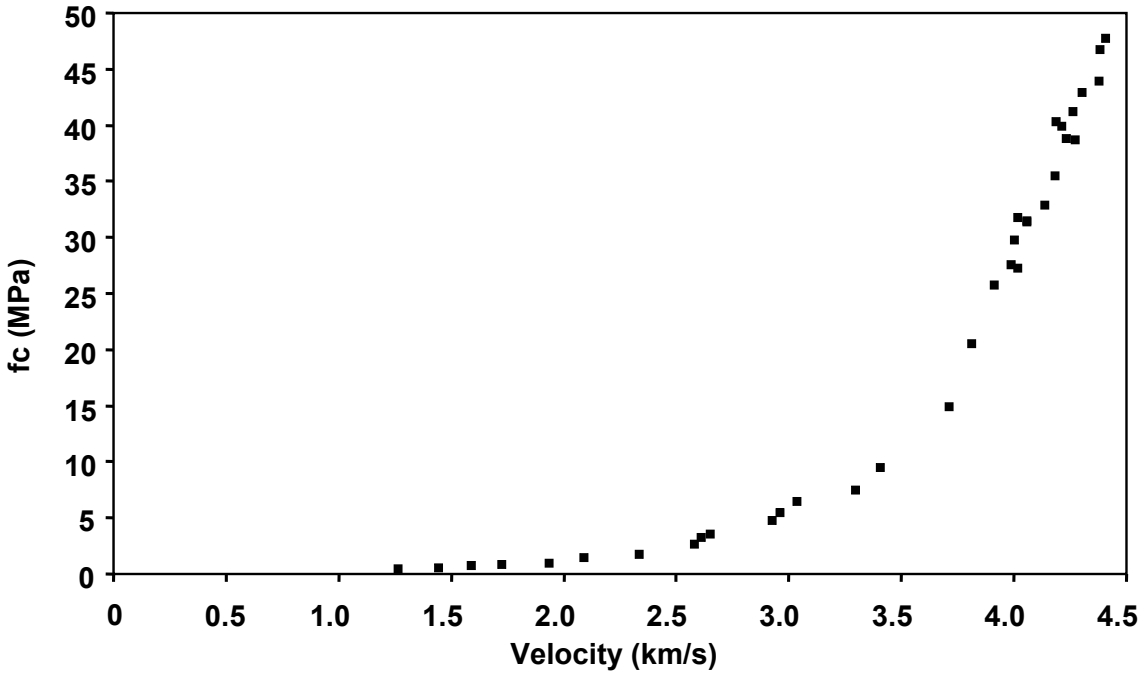

Figure 2.5 – Typical strength-velocity data

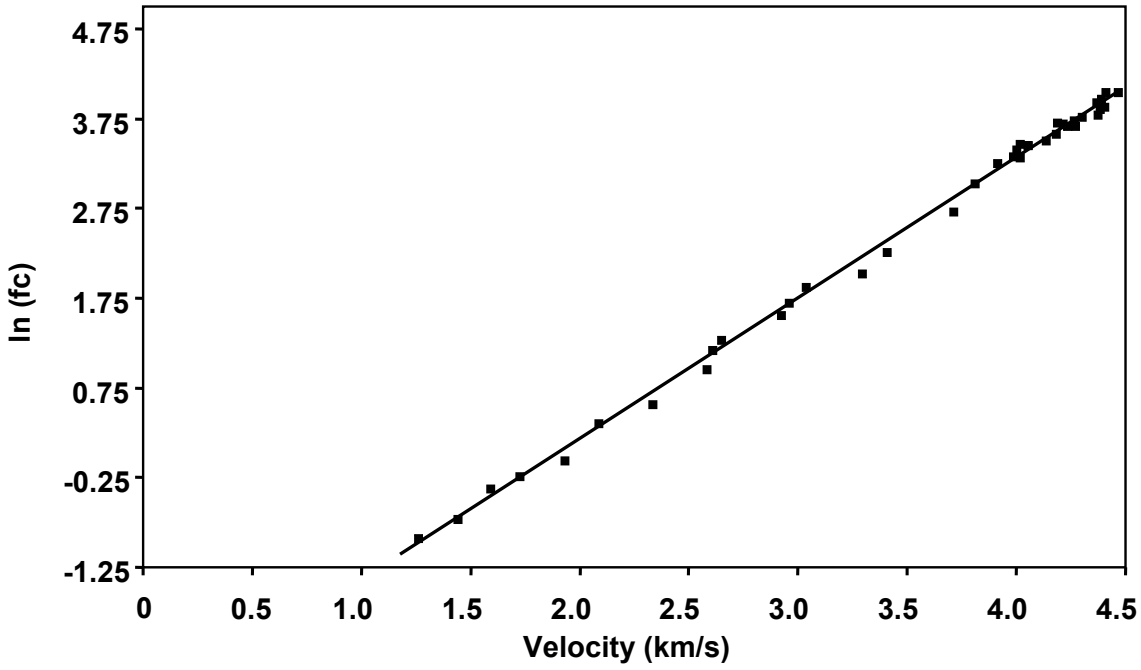

Figure 2.6 – Natural log of strength versus velocity data

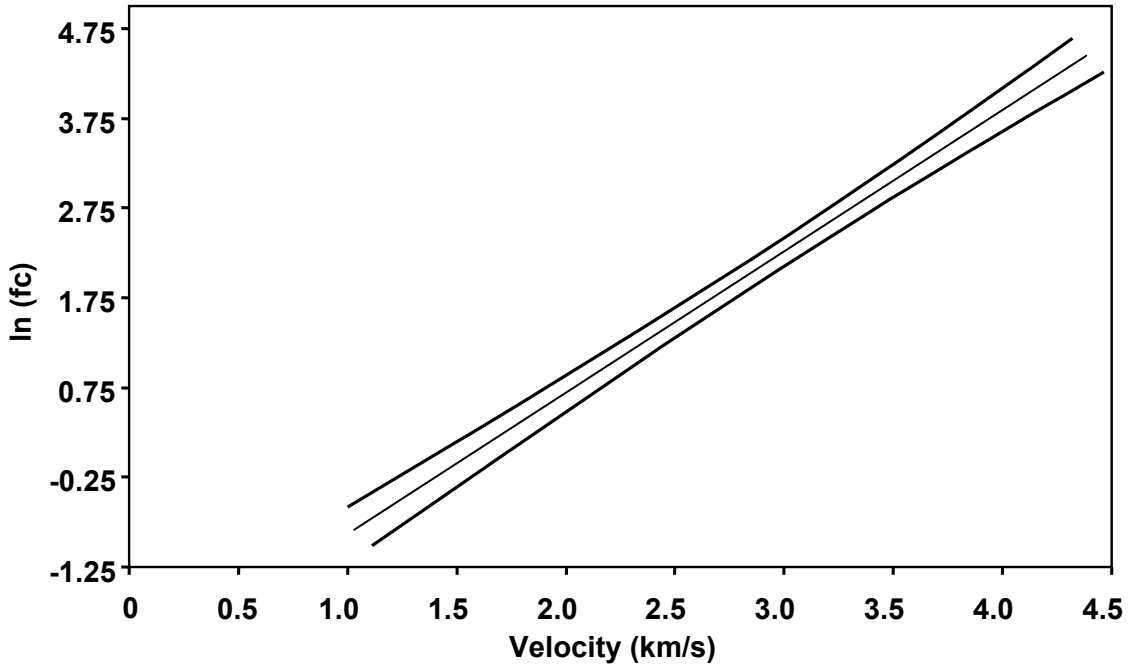

Figure 2.7 – 95% confidence limits for natural log of strength versus velocity data

CHAPTER 3

EXPERIMENTAL PROGRAM

3.1 INTRODUCTION

This chapter explains the experimental program. As explained briefly in Chapter 1, the research involved impact-echo tests and compression tests of concrete cylinders from several batches of concrete. Section 3.2 explains the test matrix used in the research. This is followed by Section 3.3 which describes how test specimens were prepared and handled. Finally, Section 3.4 describes the specimen testing procedure.

3.2 TEST MATRIX

Table 3.1 contains basic information about the concrete mixtures that were tested in the experiments. The first column, Mixture Type, has Arabic Numerals to denote which batches share the same basic ingredient proportions. The second column, Mixture ID, has an individual identification number for each batch of a given Mixture Type. The format for the ID is YYMMDDN, where YY is the last two digits of the year of start of the test, MM is the month, DD is the day, and finally N is an "A" or "B" suffix to separate data when the testing of two batches began on the same day. For example, 030108A was a batch whose testing began on January 8, 2003, and 030108B was the other batch whose testing began on that same day. The next several columns list the proportions of ingredients for each batch. The Set-Controlling Admixture column lists any set-controlling admixtures added to the batch. The last column, Comments, contains any other pertinent information about the batch.

Repeated batches of Type 1 mixtures were used to test the effectiveness of the method developed to estimate the rate of strength gain. As stated in Chapter 2, factors such as the volume fraction of aggregate influence the strength-velocity relationship, therefore it was critical to use mixtures with the same volume fraction of aggregate in these tests. Tests were performed on Type 1 mixtures with the addition of admixtures to alter the setting times. These alterations were used to test the accuracy of the method for predicting rate of strength gain. The 030214B batch deserves special comment. In order to greatly slow the curing rate, and therefore evaluate the method of predicting rate of strength gain under a more extreme case, the cylinders from this batch were placed in an ice-water bath during the initial stage of testing.

Figure 3.1 shows the temperature versus age data from the seven batches that were tested. Figure 3.1 (a) contains the data from the three batches tested in August, 2002. The 020808A and 020812A batches both contained a retarding admixture and exhibit similar temperature versus age data. The 020812B batch had no retarding admixture and reached

its peak temperature sooner than the other two batches. Figure 3.1 (b) contains the data from the batches tested in January, 2003. It can be noted from this figure that the Type 1 and Type 2 mixture exhibited similar temperature versus age behavior. Figure 3.1 (c) contains the data from the two batches tested in February, 2003. The effects of the ice-water bath on the curing temperature of the 030214B batch are apparent.

The Type 2 mixture was used to test the effectiveness of the impact-echo method as a quality control tool. This mixture had a different volume fraction of aggregate, and therefore a different strength-velocity relationship than the Type 1 mixtures. The statistical analysis described in Chapter 2 was used to determine whether this difference was detectable by comparing the impact-echo data from the Type 1 and Type 2 mixtures. The results of this analysis are presented in Chapter 5.

3.3 SPECIMEN PREPARATION AND HANDLING

A large number of concrete cylinders, typically around 50 for each batch were prepared to fully populate the strength-velocity curve. Included in Table 3.1 is the total number of cylinders tested for each batch. These cylinders were 152mm x 305mm (6 inch x 12 inch) in size and were cast in plastic cylinder molds. The large quantity of cylinders was due to a need for almost constant testing throughout the first 24 hours from the pour, and after 24 hours, enough cylinders for two tests at 36 hours, three days, seven days, fourteen days, and 28 days. Figure 3.2 is a photograph of cylinders being prepared for testing.

The earliest tests were made when the concrete had a compressive strength as low as 0.24 MPa (35 psi). At these low strengths the cylinders were damaged when stripped using a traditional stripping tool. To avoid damage, several of the cylinder molds were pre-cut as shown in Figure 3.3. Basically, the mold was cut in half longitudinally and put back together using duct tape. To strip these cylinders the duct tape was removed and the mold was pulled apart, releasing the cylinder. In general, once the concrete strength reached about 1.03 MPa (150 psi), the cylinders could be removed from the molds using traditional stripping methods without causing damage to the cylinders.

Once the cylinders were prepared, they were covered by a plastic tarp to reduce moisture loss. Except for the ice-water chilled mix, the cylinders were allowed to cure in the same manner that the cylinders for the structural members in a precast plant are cured. A thermocouple was placed in one cylinder from each concrete batch to record the temperature changes from curing.

In an attempt to further curtail moisture loss, a thin plastic bag was placed over the cylinder being tested. This bag remained in place during the impact-echo testing and was removed when the cylinder was tested in compression. Several tests on August 8, 2002 confirmed that the plastic bag had no influence on the impact-echo test result, so all tests thereafter were made with a bag on the cylinders.

At ages less than 24 hours, all cylinders were kept in their molds until being readied for a test. After roughly 16 hours, the plastic tarp covering all of the remaining cylinders was removed, and the cylinders, still in their molds, were covered with a plastic cap to retain moisture. After roughly 24 hours the cylinders were transported from the precast plant to the laboratory, stripped from the molds and placed in a lime-water bath as per ASTM standards. The cylinders were kept in the lime-water baths through the final tests at 28 days, at which time the testing was completed for a concrete batch.

3.4 SPECIMEN TESTING

Impact-echo tests were performed by dropping a 4.69mm steel sphere onto the end of a cylinder. A 150mm (5.91 inch) tall PVC tube was used to control the drop height and position on the cylinder. Figure 3.4 shows the impact-echo equipment on a cylinder, with key components identified. The displacement transducer provided a voltage output proportional to the normal surface displacement. The voltage output from the displacement transducer was captured and recorded by a digital processing oscilloscope. The oscilloscope was capable of directly performing the fast Fourier transformations and storing the displacement waveforms and amplitude frequency spectra to a computer disk. Figure 3.5 shows the digital processing oscilloscope and a cylinder ready to be tested by the impact-echo method.

In this research a complete test of one cylinder was comprised of performing an impact-echo test, recording the P-wave frequency and the time of the test, and then testing the cylinder in compression and recording the compressive strength. Figure 3.6 shows a cylinder being tested in compression. The impact-echo equipment was juxtaposed with the compression testing machine. This allowed the compression test to be performed within a minute of the impact-echo test.

During the initial curing period for the cylinders, data collection intervals were chosen based on P-wave frequencies that would evenly populate the velocity versus age curves, and was often limited by the time needed to test a cylinder in compression. As the curing rate slowed and after 24 hours, tests were performed on an age basis. Testing at the laboratory consisted of the same methods utilized during testing at the precast plant.

Mixture Type	Mixture ID	Grey Cement (kg)	Slag (kg)	Fly Ash (kg)	Coarse Aggregate (kg)	Fine Aggregate (kg)	Water (kg)
1	020808A	299	0	64	726	560	127
1	020812A	299	0	64	726	560	127
1	020812B	299	0	64	726	560	127
1	030108A	299	0	64	726	560	127
2	030108B	265	177	0	794	432	122
1	030214A	299	0	64	726	560	127
1	030214B	299	0	64	726	560	127

Mixture Type	Mixture ID	Air Entraining Admixture (mL)	Pozzolan (mL)	Water Reducing Admixture (mL)	Corrosion Inhibitor (mL)	Set-Controlling Admixture	Number of Cylinders Tested	Comments
1	020808A	148	0	2218	11356	Retarding	37	
1	020812A	148	0	2218	11356	Retarding	39	
1	020812B	148	0	2218	11356	None	41	
1	030108A	222	0	2366	11356	Accelerating	42	
2	030108B	606	414	3549	11356	Accelerating	36	High strength slag mixture
1	030214A	222	0	2366	11356	Accelerating	35	
1	030214B	222	0	2366	11356	Accelerating	26	Cured in ice-water bath

Table 3.1 - Concrete mixture data

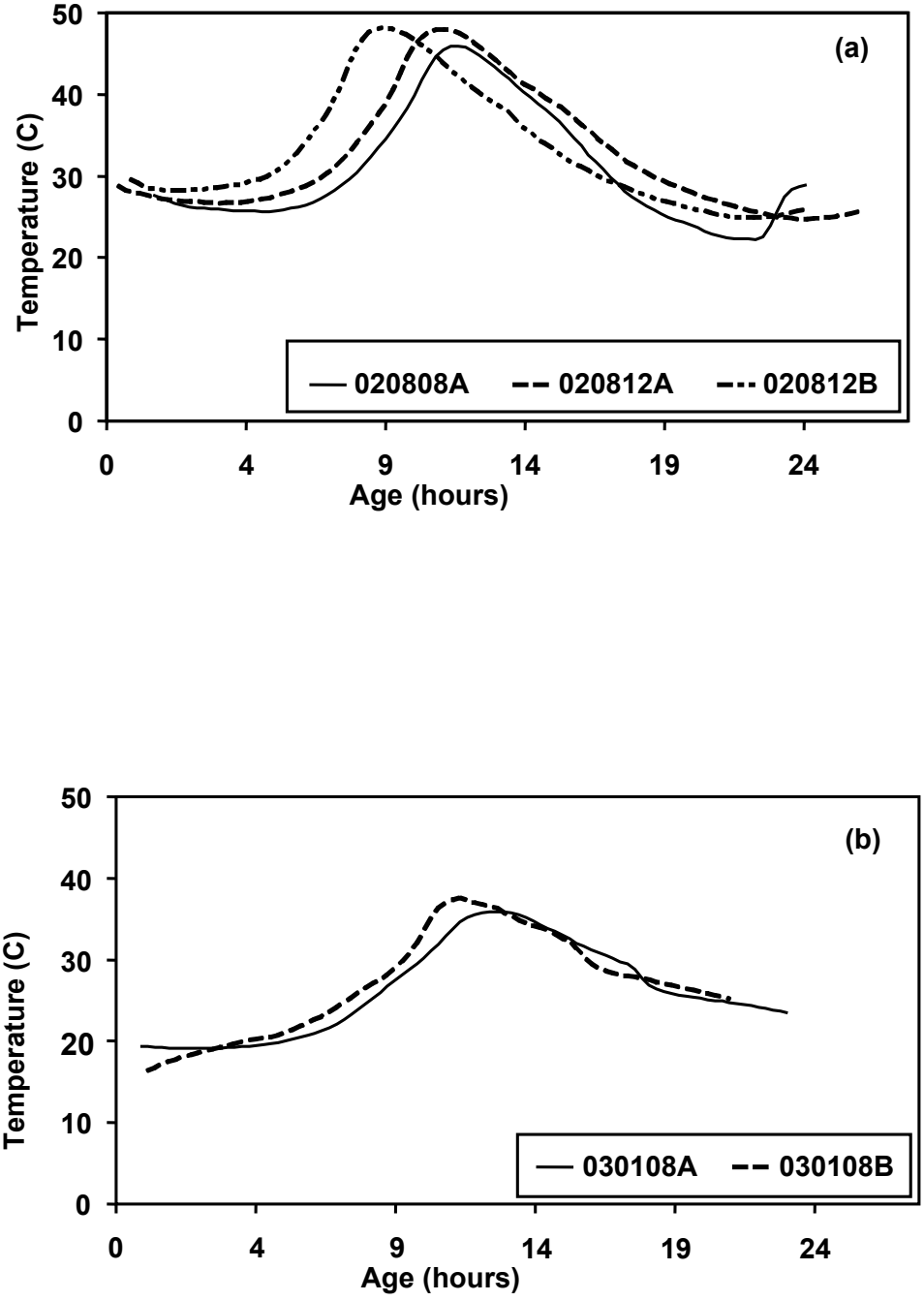

Figure 3.1 – Temperature versus age data for test specimens

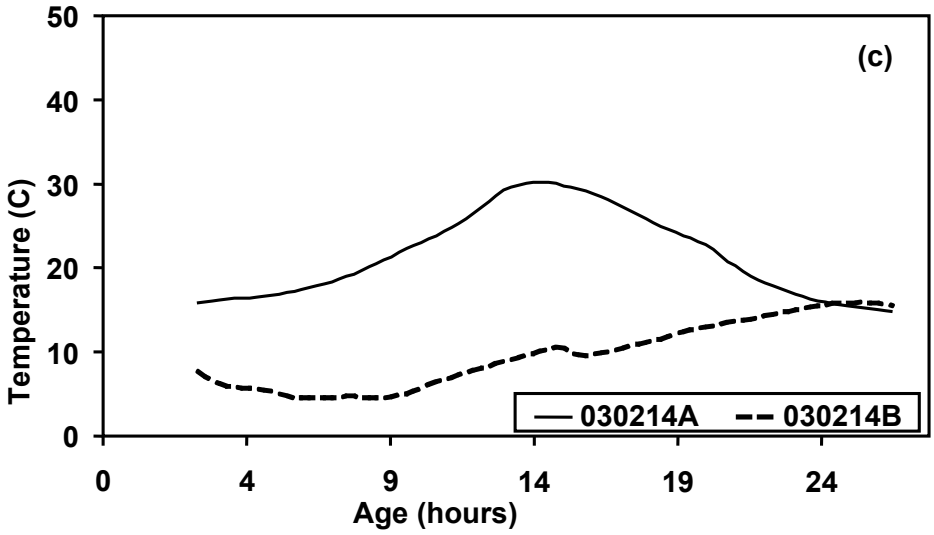

Figure 3.1 (continued) – Temperature versus age data for test specimens

Figure 3.2 – Preparation of cylinder specimens in the precast plant

Figure 3.3 – Pre-cut cylinder mold for early-age strength tests

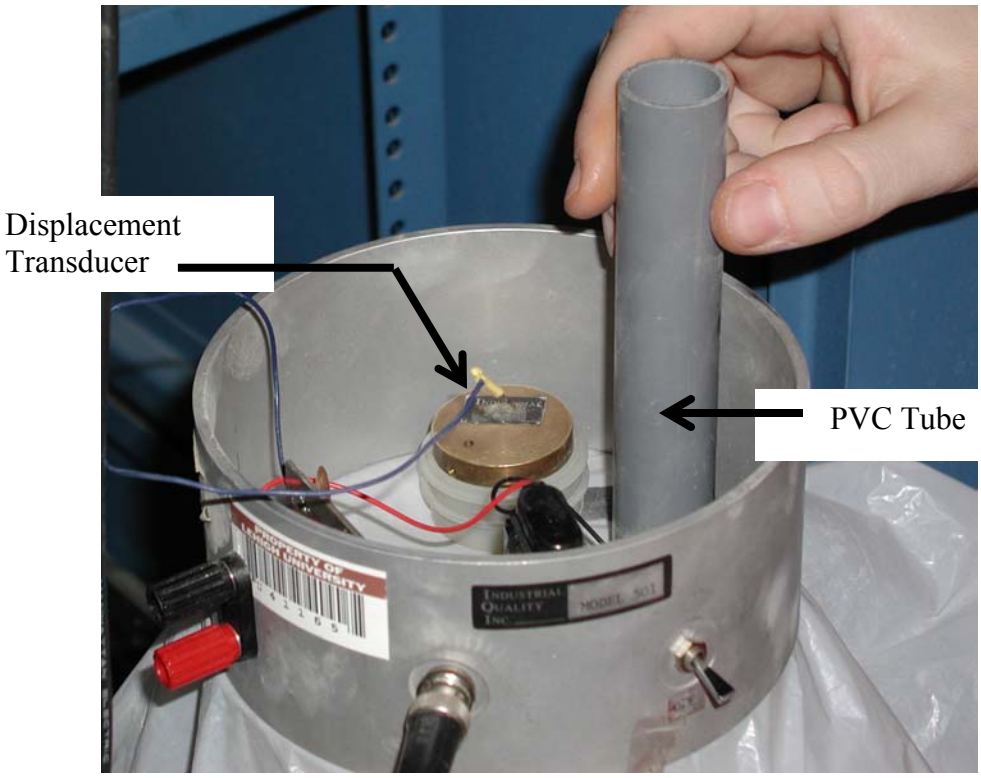

Figure 3.4 – Impact-echo equipment set up on a cylinder for testing

Figure 3.5 – Digital processing oscilloscope and cylinder ready for testing

Figure 3.6 – Cylinder being tested in compression

CHAPTER 4

INTERPRETATION OF RESULTS FROM A TYPICAL EXPERIMENT

4.1 INTRODUCTION

This chapter explains how the results from a typical experiment are interpreted. The data used for this purpose was collected from a Type 1 concrete mixture, specifically that of the 020812A batch. First, a table with the data through 36 hours is given, along with several plots of the surface displacement waveform and corresponding spectra. Then plots of strength versus age, velocity versus age, strength versus velocity, natural log of strength versus velocity, and natural log of strength versus age are shown. The data and plots show the changes and trends in the impact-echo data that occur as the concrete mixture cures.

4.2 DATA FROM THE 020812A MIXTURE

Table 4.1 contains all of the data of interest from the 020812A batch up to 36 hours from the pour. As stated in Chapter 2, the impact-echo method is more useful at early ages when the velocity is changing rapidly relative to strength. Therefore, the data is cut off after this point. This range of data also contains the point at which the transfer strength specified by the precast plant was reached. The first column in the table is age, in hours. This is the time period between when the concrete mixture was poured and when the data point was collected. For example, the first data point was collected 7.33 hours after the concrete mixture was poured. The second column is velocity, in kilometers per second, of the P-wave. The third column is the compressive strength of the concrete in MPa. The fourth column is the natural log of the compressive strength.

Figures 4.1 and 4.2 are a series of plots of the surface displacement waveforms and the frequency amplitude spectra from several of the impact-echo tests performed on the specimens from the 020812A batch. These plots represent typical output from an impact-echo test. Typical P-wave arrivals are identified on the waveforms. Note that the P-wave arrivals identified are not 2P, 4P, and so on. Two successive arrivals are identified in a manner to maintain clarity on the figures. Also noted in the surface displacement waveforms is a low frequency oscillation. This is the response of the transducer at its own natural frequency. The P-wave frequencies are noted on the spectra. The peak occurring at a frequency of about 0.75 kHz is the resonant frequency of the displacement transducer. The time interval between P-wave arrivals decreases as the concrete cures, and is reflected by the closer spacing of the P-wave arrivals on the waveform. It is also seen by the increase in the frequency of the P-wave peak in the spectra plot.

Each point in Figures 4.3 through 4.7 represents the results of an impact-echo test and a compression test of one cylinder. Figure 4.3 shows the strength versus age data for the

020812A batch through 36 hours from the pour time. It is clear from the figure that a majority of the rapid strength gain occurred from 10 through 15 hours from the pour time. The batches tested were intended to cure at a rate to gain sufficient strength to transfer the prestress forces at 16 to 18 hours from the pour time.

Figure 4.4 shows the velocity versus age data for the 020812A batch through 36 hours from the pour time. As stated in Chapter 2, the P-wave velocity begins to exhibit less change as the age of the concrete specimen increases. In this particular case, after approximately twelve hours, the P-wave velocity starts to show this trend.

Figure 4.5 shows the strength versus velocity data for the 020812A batch through 36 hours. As discussed in Chapter 2, it is simpler to generate the equation relating strength and velocity if the natural log of strength is plotted against velocity. The results are a straight line graph as shown in Figure 4.6. Also discussed in Chapter 2, a regression line is calculated based on this plot and the equation of this line can be used to obtain the exponential equation relating strength and velocity.

Superimposed on Figure 4.6 is the best-fit straight line to the data plotted as natural log of strength versus velocity. Superimposed on Figure 4.5 is the exponential equation obtained from the parameters of the best-fit line.

Once the exponential equation relating compressive strength and P-wave velocity has been determined for a concrete mixture, it can be used in conjunction with impact-echo testing to determine when the target strength is reached, and thus when a cylinder is ready to be tested in compression to verify this. This can eliminate some of the guesswork that is currently involved in a precast plant, where a cylinder is tested in compression when it is believed that the target strength has been reached. If this is found not to be true, another cylinder is tested in compression after the concrete has been given more time to cure. It is possible that a precast plant may run out of cylinders before one is found to meet the target strength. The non-destructive nature of impact-echo testing can eliminate such a situation since no cylinders would be broken in a compression test until the impact-echo results show that the target strength is reached.

To take the issue just discussed one step further, problems with quality control could be a factor when a concrete mixture is not behaving as expected. Chapter 5 investigates using the impact-echo method for quality control. Additionally, Chapter 6 investigates using the impact-echo method to measure the rate of strength gain, namely when a target strength will be reached.

The age, P-wave velocity, and strength data from all concrete batches is presented in Appendix A.

Finally, shown in Figure 4.7 is a plot of the natural log of strength versus age data through 36 hours. This relationship is utilized in Chapter 6 to predict the time that the concrete will reach a particular target strength. This relationship can be approximated to

be a bi-linear plot. Predicting time to reach a target strength involves fitting a regression line to the bi-linear plot and using its equation along with the desired target strength to solve for the time. This concept is discussed in detail in Chapter 6.

Age (hours)	Velocity (km/s)	fc (MPa)	ln (fc)
7.33	1.266	0.39	-0.94
7.55	1.444	0.49	-0.72
7.73	1.593	0.68	-0.38
7.88	1.727	0.78	-0.25
8.03	1.935	0.93	-0.08
8.18	2.092	1.41	0.35
8.32	2.613	3.17	1.15
8.43	2.338	1.76	0.56
8.57	2.583	2.58	0.95
8.85	2.651	3.56	1.27
9.00	2.963	5.41	1.69
9.15	2.926	4.68	1.54
9.40	3.038	6.44	1.86
9.60	3.298	7.46	2.01
9.98	3.410	9.46	2.25
10.20	3.715	14.88	2.70
10.63	3.812	20.43	3.02
10.97	3.916	25.73	3.25
11.23	3.990	27.56	3.32
11.62	4.020	27.19	3.30
12.00	4.006	29.75	3.39
12.33	4.057	31.34	3.44
12.77	4.020	31.70	3.46
13.28	4.057	31.46	3.45
13.90	4.139	32.80	3.49
16.00	4.184	35.48	3.57
20.00	4.236	38.77	3.66
24.00	4.214	39.87	3.69
24.00	4.273	38.65	3.65
36.00	4.266	41.21	3.72
36.00	4.192	40.24	3.69

Table 4.1 - Results from 020812A batch

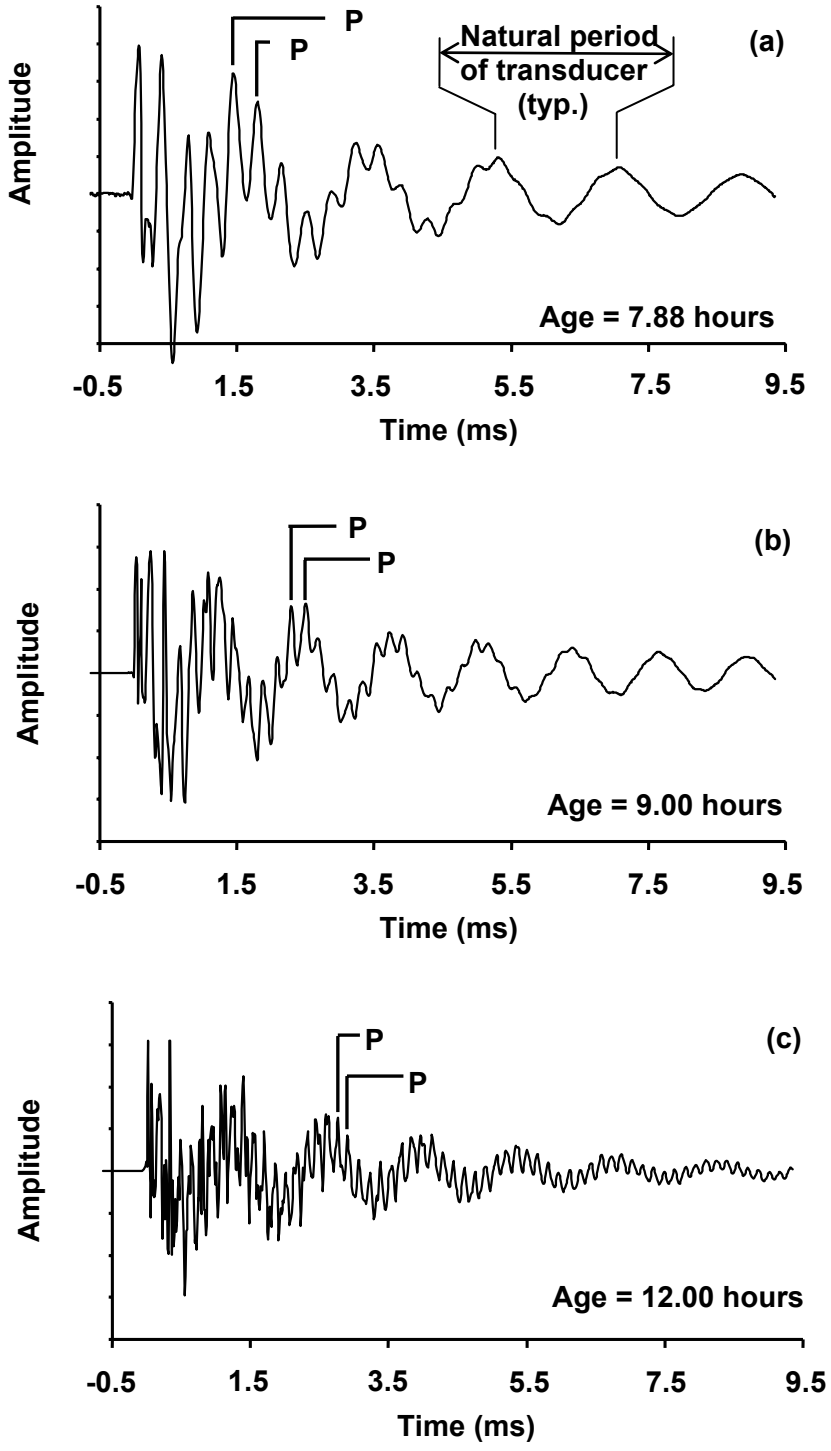

Figure 4.1 – Typical surface displacement waveforms from the 020812A batch

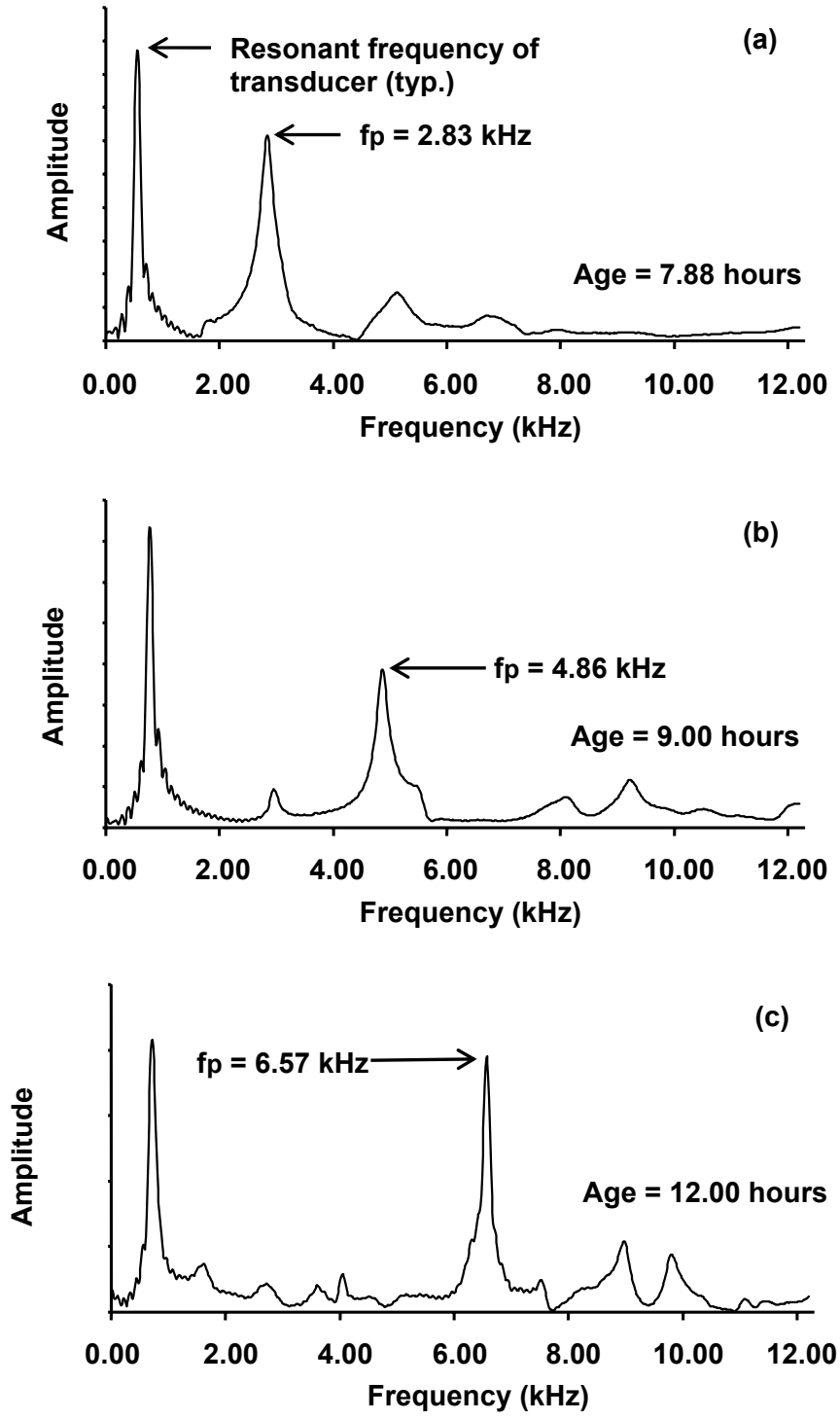

Figure 4.2 – Typical spectra data from the 020812A batch

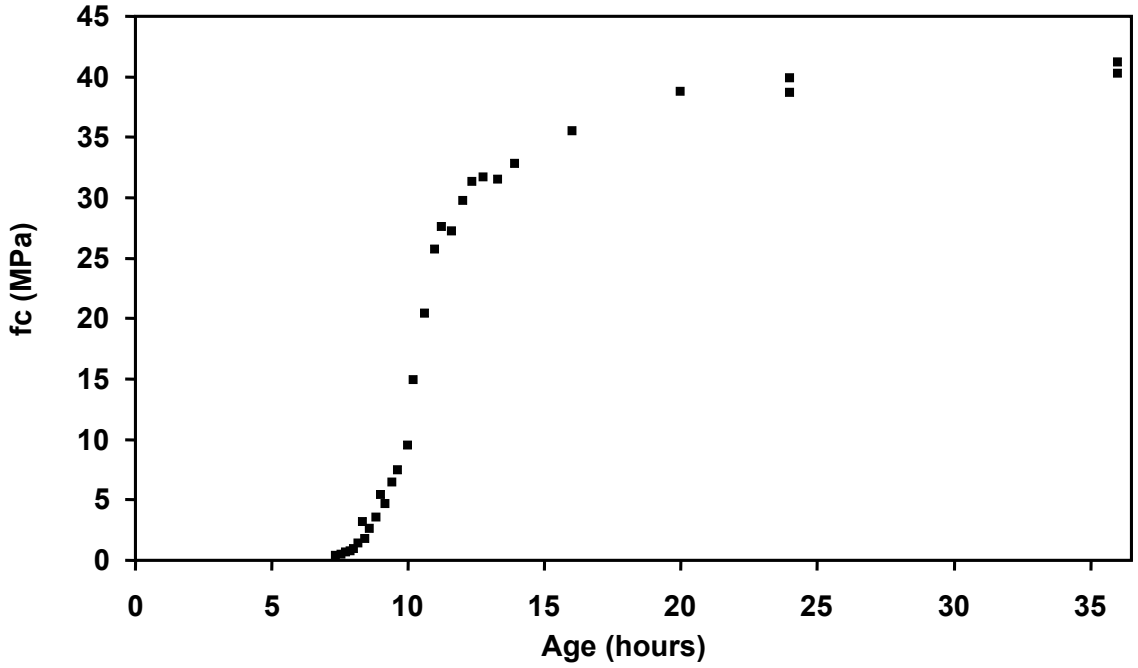

Figure 4.3 – Strength versus age data, 020812A batch

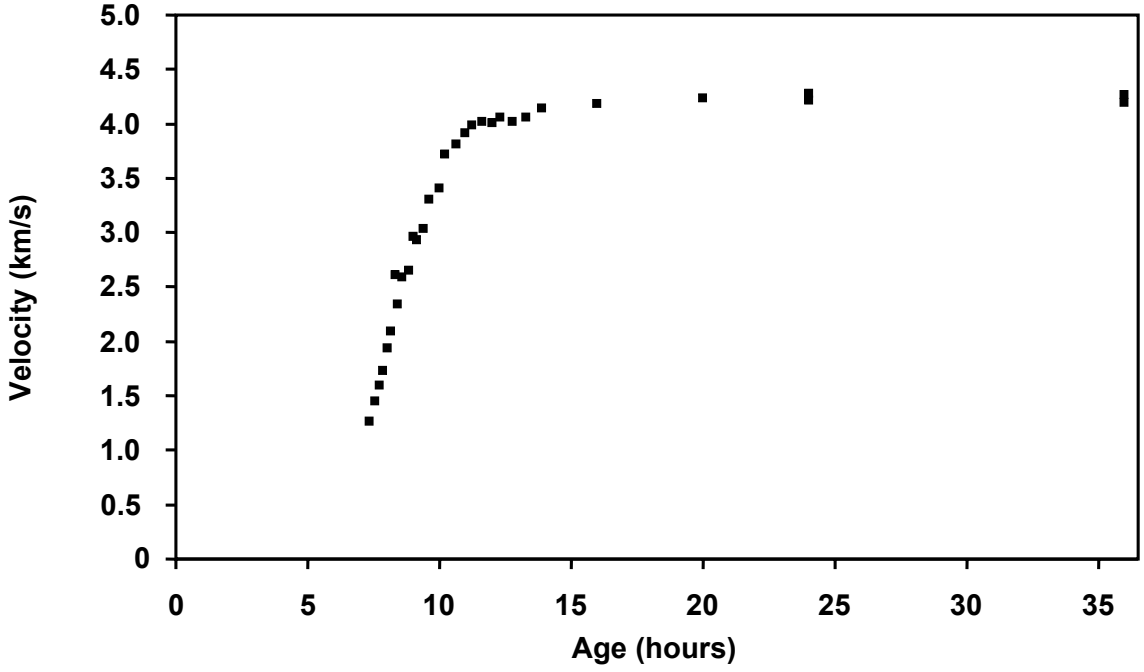

Figure 4.4 – Velocity versus age data, 020812A batch

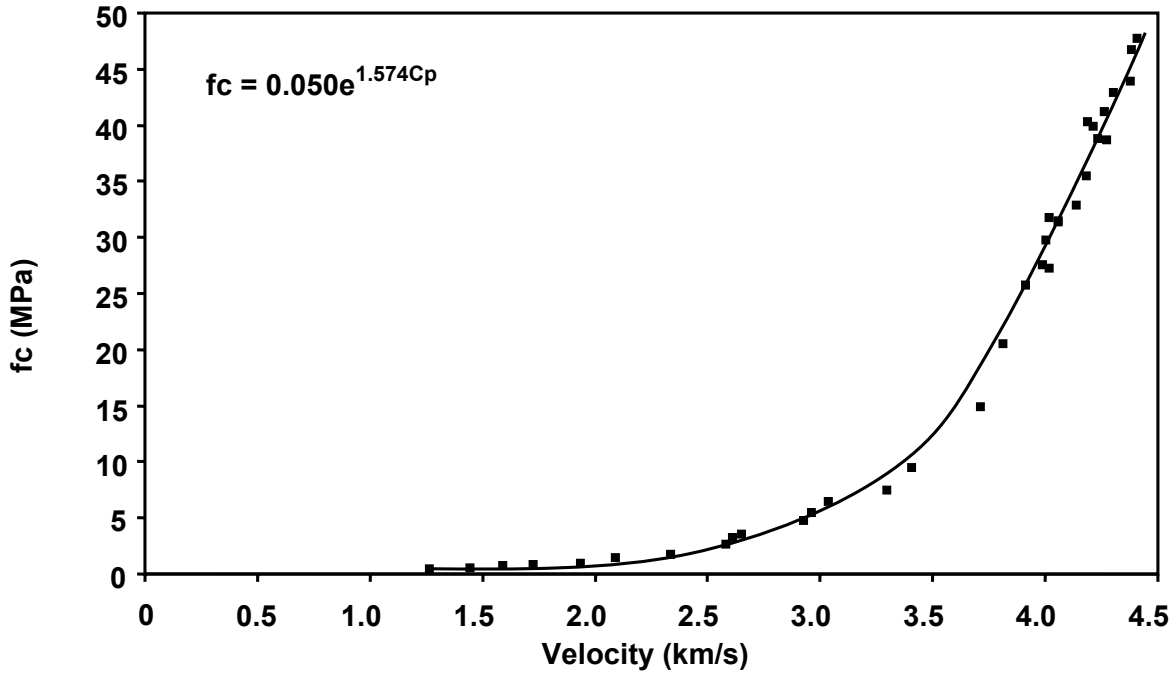

Figure 4.5 – Strength versus velocity data, 020812A batch

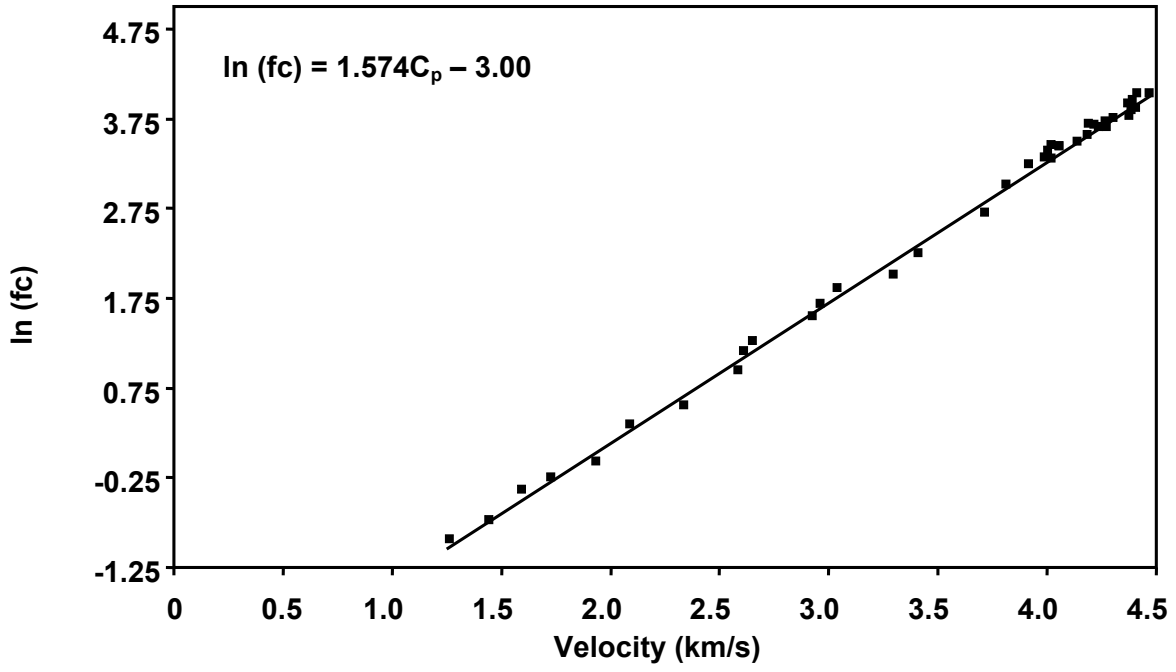

Figure 4.6 – Natural log of strength versus velocity data, 020812A batch

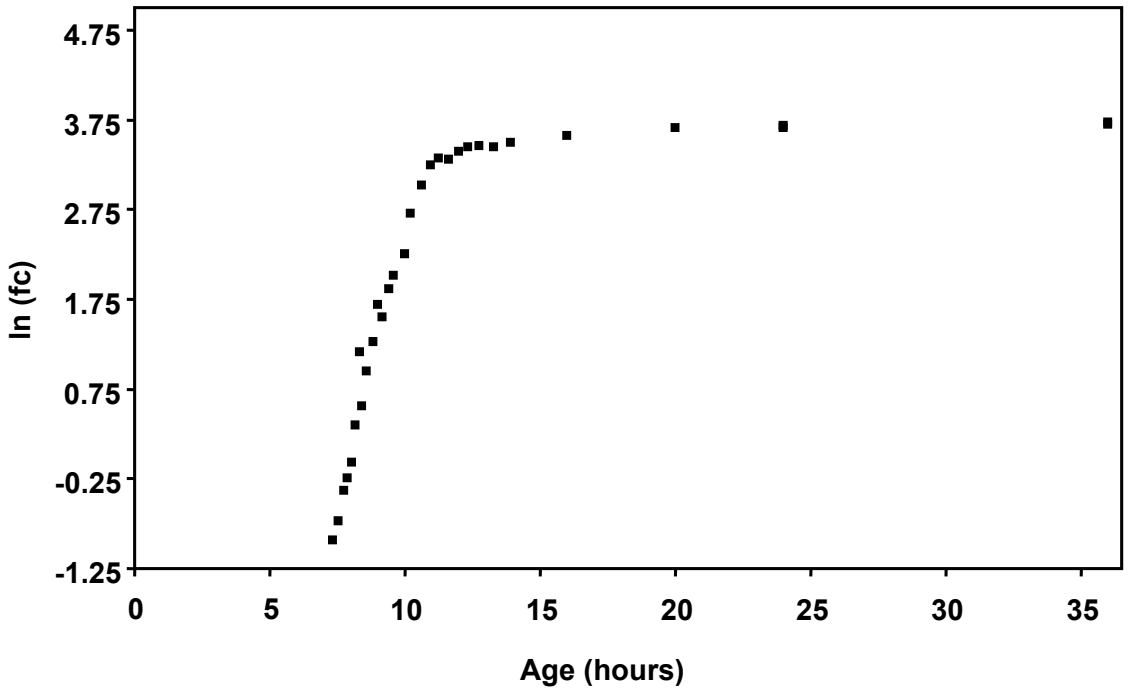

Figure 4.7 – Natural log of strength versus age data, 020812A batch

CHAPTER 5

USE OF THE IMPACT-ECHO METHOD FOR QUALITY CONTROL

5.1 INTRODUCTION

This chapter examines the first objective stated in Chapter 1, namely the use of the impact-echo method as a tool for quality control of concrete mixtures in a precast plant. The basic premise is as follows: the strength-velocity relationship of a given mixture is a measure of the performance of the mixture, especially at early ages. An unintended change in the quality or quantity of the constituent ingredients for a given concrete mixture may alter the strength-velocity relationship in a statistically measurable way. If routine impact-echo testing is performed to assist in decisions about when to test cylinders in compression or to predict the time when the transfer strength is obtained (Chapter 6), then a strength-velocity result that deviates from the established strength-velocity relationship can alert quality control personnel about a possible unintended change in the quality or quantity of constituent materials.

The approach taken in this research is to calculate confidence limits for a strength-velocity relationship and compare impact-echo results to these confidence limits. Data that fall outside of the confidence limits are indicators that the concrete mixture is behaving differently than the concrete mixture used to establish the strength-velocity relationship.

Section 5.2 gives an example for calculating a confidence limit based upon data from the six batches of the Type 1 concrete mixtures that were tested. Section 5.3 shows the results of testing the confidence limits with a concrete mixture (Type 2) that is known to have a different composition of ingredients. Then, Section 5.4 presents a suggested method for using impact-echo testing for quality control. Lastly, Section 5.5 presents conclusions on this part of the research.

5.2 EXAMPLE FOR CALCULATING A CONFIDENCE LIMIT

As stated in Chapter 3, six of the seven tests performed in this research utilized the same concrete mixture, and are designated as Type 1 mixtures. The mixtures were batched with the same ingredient proportions, and therefore any deviations would presumably be due to the accuracy of the batching operation and the resolution of the impact-echo equipment.

Figure 5.1 shows the natural log of strength versus velocity results from the six batches that tested the Type 1 concrete mixture. Since the impact-echo method becomes less sensitive at later ages and the transfer strength requirements for the precast plant is 24.1

MPa (3500 psi), the data considered includes all points below 27.6 MPa (4000 psi). This contains the strength range of interest, avoids biasing the results based on data from later ages, and keeps the data within the more sensitive range of strength estimation for the impact-echo method.

The formula for developing confidence limits given in Chapter 2 calculates a pair of points, upper and lower, for any given x_o value, where x_o is the P-wave velocity. Therefore to generate confidence limits to encompass the entire set of data, the calculations are repeated for x_o values that encompass the entire range of data. To illustrate the calculations, a single pair of points (i.e. the upper and lower points on the confidence limit) is calculated here for the x_o value of 3.000, which is a random point from the series of x_o values used to form the confidence limits. The calculations are summarized in Table 5.1 and are explained below. The data for all of the statistical calculations is given in Table 5.2.

The first step to calculating the confidence limits is to fit a mean to the log of strength versus velocity data for all Type 1 batches. The confidence limits are calculated in reference to this mean. Figure 5.2 shows the data fitted with a mean. The equation for the mean line was calculated to be:

$$y = 1.610x_o - 3.118 \qquad (5.1)$$

Inserting the x_o value of 3.000 into Equation 5.1 yields the value corresponding to $\mu_{Y|x_o}$ of 1.713 in Equation 2.10.

The next step is to calculate the values for the other variables listed in Equation 2.10. The data set contained 120 points, which is the value for n. The $t_{\alpha/2,n-2}$ value taken from a table of t-distribution values in Montgomery and Runger (1994), for n-2 points and a 95% confidence limit is 1.98. The standard error, σ^2, is calculated as 0.748. The mean x value, or $\bar{x}$, is 2.7. S_{xx} is 89.7 and 3.000 is the value for x_o.

The final step to calculate a pair of confidence limits is to substitute all of the variables into Equation 2.10. The upper confidence limit, calculated with the positive value for the second term, is 1.876 and the lower confidence limit is 1.550. These two points are plotted. Repeating this calculation for all x_o values produces Figures 5.3 and 5.4.

5.3 TESTING 95% CONFIDENCE LIMITS WITH A KNOWN VARIANT

One of the concrete mixtures tested was specifically selected because of its differing material composition, which was expected to yield a different strength-velocity relationship. This mixture was the 030108B batch, and was designated a Type 2 mixture. This section shows the results of comparing the data from this mixture with the 95% confidence limits calculated in the previous section.

Figure 5.5 shows the natural log of strength versus velocity results for the one Type 2 concrete mixture. Superimposed on the results is the mean line fitted to the results.

Figure 5.6 shows the mean of the Type 2 mixture, the mean of the six Type 1 mixtures and the 95% confidence limits based upon the six Type 1 mixtures.

Note that Figure 5.6 shows that the mean for the Type 2 mixture crosses outside of the 95% confidence limits for the Type 1 mixture. Based on the data collected, this is a result of the Type 2 mixture having a different strength-velocity relationship than the Type 1 mixture. This shows that the impact-echo method can distinguish between different mixtures. It is reasoned that the impact-echo method can therefore also identify if the performance of a mixture changes over time. Therefore, the impact-echo method has the potential to be used as a quality control tool.

5.4 SUGGESTED USE OF THE IMPACT-ECHO METHOD FOR QUALITY CONTROL

The results gathered from the experiments can be used to create an initial set of guidelines for using the impact-echo method for quality control. These guidelines are a proposal and need to have additional testing performed to verify their validity.

Confidence limits for a mixture of interest can be calculated using the methods described in this report and in conjunction with strength-velocity data collected from the impact-echo method, also as per the methods described in this report. The precast operations can then use the strength-velocity relationship to nondestructively determine strength for day-to-day operation. If a supplier for a mixture ingredient changes, tests should be performed to determine the strength-velocity relationship of the mixture with the new ingredient. If the mean for this strength-velocity relationship crosses or completely lies outside of the established confidence limits, a new strength velocity relationship should be created based on the current form of the mixture. This will ensure that the accuracy of the predicted strength remains good. Periodic tests to determine the strength-velocity relationship should be made even if the ingredient suppliers do not change in order to ensure the ingredients are consistent. Results from day-to-day operations can also be used for this purpose.

5.5 CONCLUSIONS

Previous research, discussed in Chapter 2, has shown that variations in the ingredient portions of a concrete mixture can influence the relationship between compressive strength and P-wave velocity.

Confidence limits were calculated for the mean of the natural log of strength versus P-wave velocity data from several experiments utilizing the same concrete mixture. When data from a concrete mixture with differing ingredients was superimposed on these confidence limits, it crossed outside of the confidence limits. Therefore, confidence

limits can be used in combination with the impact-echo method to monitor deviations in the ingredients of a concrete mixture.

If precast concrete companies use the impact-echo method to nondestructively evaluate concrete strength, confidence limits should be calculated for the curve used to predict strength. Periodic testing should be performed to ensure that the natural log of strength versus P-wave velocity data stays within these limits, and if not, a new strength-velocity relationship should be developed in order to maintain accurate strength prediction.

Regression Coefficients:

Slope: 1.610

Y-Intercept: -3.118

$x_o = 3.000$

$\mu_{Y|x_o} = (1.610)(3.000) - 3.118$

$\mu_{Y|x_o} = 1.713$

n = 120 points

$t_{\alpha/2,n-2} = 1.98$

$\sigma^2 = 0.748$

$\bar{x} = 2.7$

$S_{xx} = 89.7$

$$\mu_{Y|x_o} \pm t_{\alpha/2,n-2}\sqrt{\sigma^2\left[\frac{1}{n} + \frac{\left(x_o - \bar{x}\right)^2}{S_{xx}}\right]} \qquad (2.10)$$

$$1.713 \pm 1.98\sqrt{0.748\left[\frac{1}{120} + \frac{(3.00 - 2.7)^2}{89.7}\right]}$$

= 1.550 (minimum 95%)

= 1.876 (maximum 95%)

Table 5.1 - Summary of calculations of a pair of points on the 95% confidence limit for the Type 1 concrete mixture

95% Confidence Limits about the Mean			
x_o	$\mu_{Y\|x_o}$	min. 95%	max. 95%
1.000	-1.507	-1.860	-1.155
1.250	-1.105	-1.418	-0.792
1.500	-0.702	-0.977	-0.428
1.750	-0.300	-0.539	-0.061
2.000	0.103	-0.104	0.310
2.250	0.505	0.325	0.686
2.500	0.908	0.745	1.071
2.750	1.311	1.154	1.467
3.000	1.713	1.550	1.876
3.250	2.116	1.935	2.296
3.500	2.518	2.311	2.725
3.750	2.921	2.682	3.160
4.000	3.323	3.049	3.598

Table 5.2 - Calculated values for 95% confidence limits

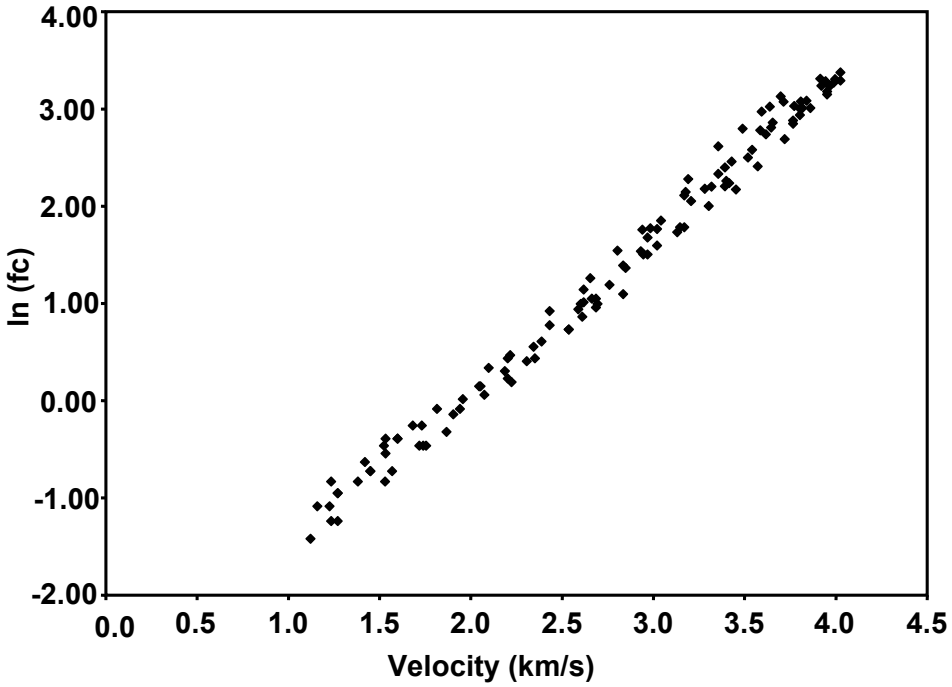

Figure 5.1 – Natural log of strength versus velocity results for all six Type 1 mixtures

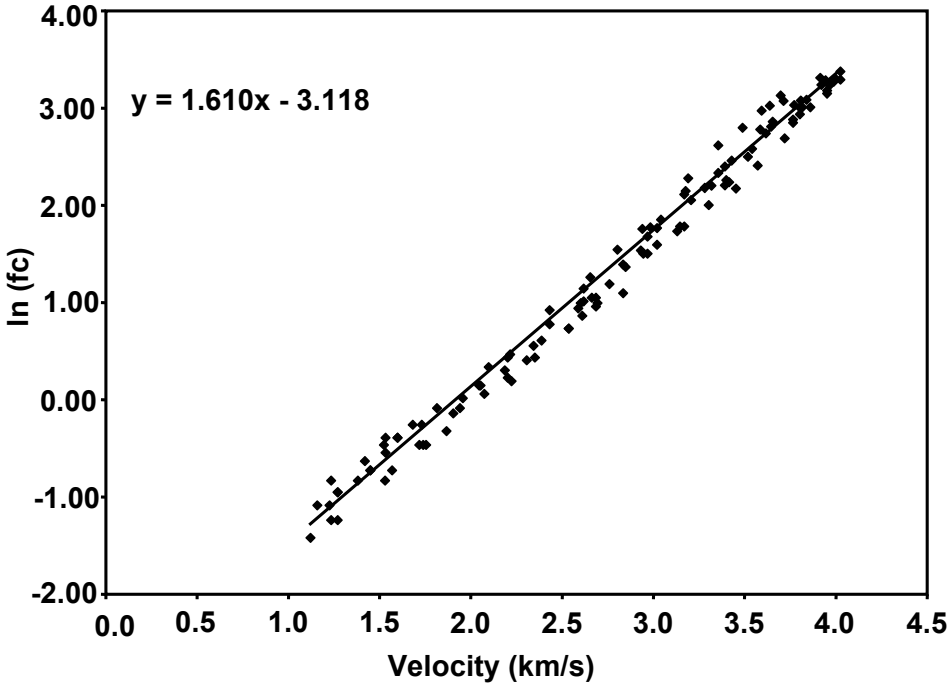

Figure 5.2 – Mean line fitted to all six Type 1 mixtures

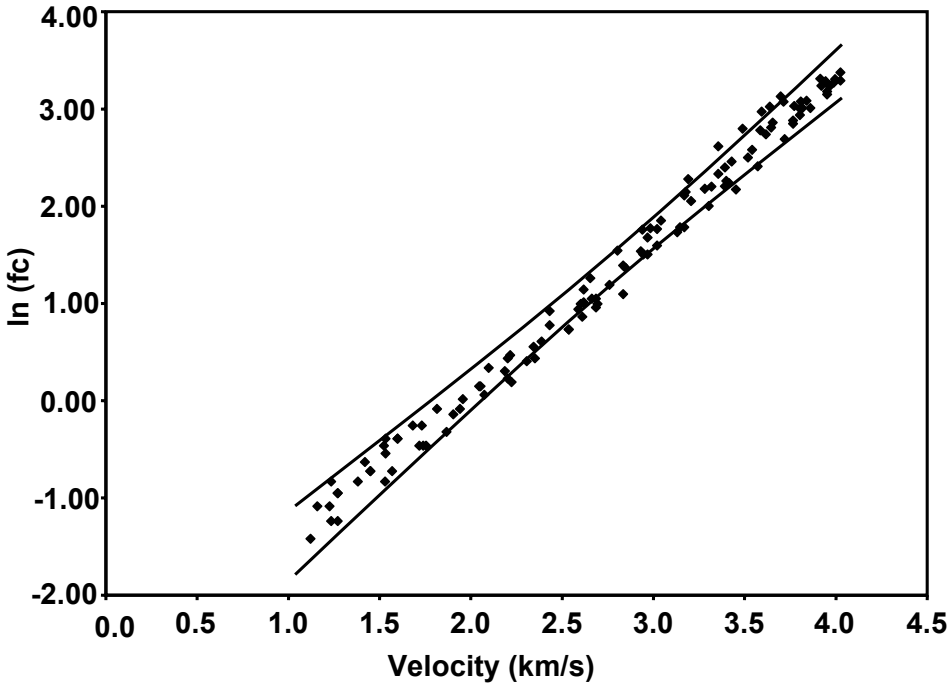

Figure 5.3 – 95% confidence limits around the natural log of strength versus velocity results for all six Type 1 mixtures

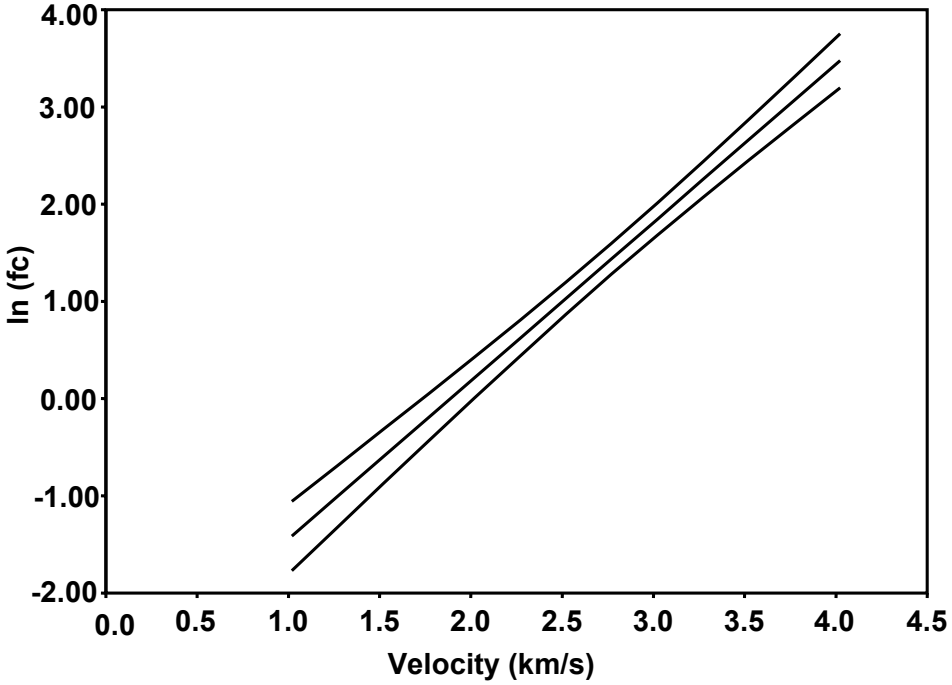

Figure 5.4 – 95% confidence limits around the mean of the results for all six Type 1 mixtures

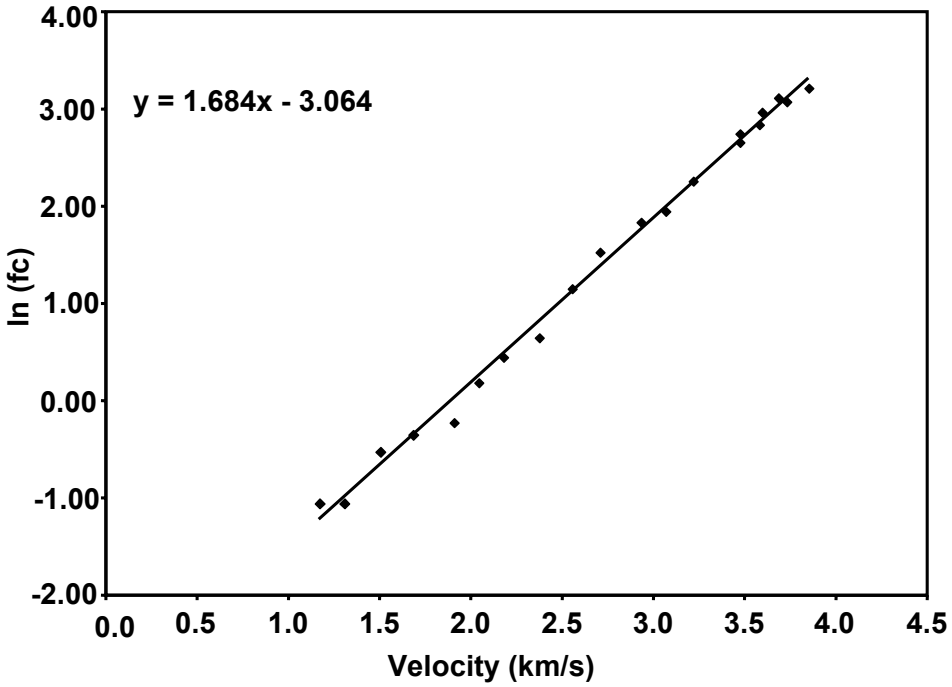

Figure 5.5 – Natural log of strength versus velocity results for the Type 2 mixture (030108B) with mean line fitted to the results

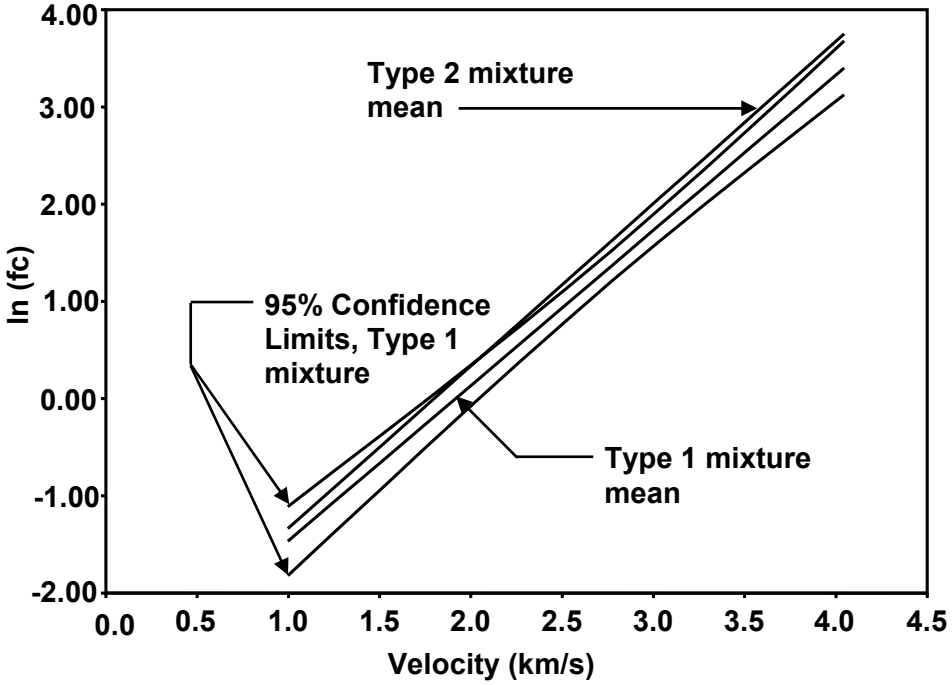

Figure 5.6 – Type 2 mixture (030108B) mean crossing outside of 95% confidence limits of all six Type 1 mixtures

CHAPTER 6

PREDICTING TIME TO REACH A TARGET CONCRETE COMPRESSIVE STRENGTH

6.1 INTRODUCTION

One advantage of the impact-echo method is that concrete strength is estimated independent of the age of the concrete. The relationship between strength and velocity is unaffected by changes in curing temperature or the use of set-controlling admixtures, both of which influence the age at which a particular strength may be attained.

As a practical matter, in precast operations, it is beneficial to be able to predict when a concrete mixture will reach a particular compressive strength (e.g. the transfer strength). This chapter examines the use of the impact-echo method as a means to predict the time when a particular concrete compressive strength will be reached.

Section 6.2 describes the general approach taken to predict the time to reach a target concrete compressive strength. Section 6.3 describes three different methods that were used and are based on the general approach discussed in Section 6.2. Section 6.4 compares the results from the three methods discussed in Section 6.3. Finally, Section 6.5 gives conclusions on using the impact-echo method to predict the time when a particular concrete compressive strength will be reached.

6.2 GENERAL APPROACH

The natural log of strength versus time relationship was described in general in Chapter 4. Figure 6.1 shows a typical plot of natural log of strength versus age through 28 days for the 030214A batch which is one of the Type 1 concrete mixtures. As shown in the figure, the relationship is approximately bi-linear. This relationship is used to develop an approach for predicting the time when a particular concrete compressive strength is reached. In this research, this target strength is denoted as $f_{c,\,target}$. This section describes the steps involved to develop this approach.

The first step in predicting the time to reach a target strength is to measure the P-wave velocity of a test cylinder with the impact-echo method. This P-wave velocity is then used in conjunction with the previously established strength-velocity relationship for the given concrete mixture to estimate the strength of the concrete. The natural log of the estimated strength and the age of the specimen are then plotted. This process is repeated with additional points being plotted as the concrete cures. Figure 6.2 shows three successive points from the 030214A batch plotted using the above procedure.

The next step in the approach is to fit a linear regression line to the data shown in Figure 6.2. Figure 6.3 is a plot of a regression line fitted to the data from Figure 6.2. Also shown in the figure is the natural log of the target strength. In this illustration, the target strength, $f_{c,\,target}$, is 0.82 MPa, and the natural log of $f_{c,\,target}$ is -0.2. The equation of the regression line is extrapolated to intersect the natural log of the target strength to predict the age when the target strength will be reached.

Limitations on this approach do exist. As shown in Figure 6.1, the first linear segment exhibits large changes in strength with small changes in time. This is the region where predicting the time of a target strength is most accurate. Therefore the natural log of the target strength must fall on this first linear segment.

6.3 TIME PREDICTION WITH DIFFERENT REGRESSION METHODS

The preceding section described the general approach utilized to predict the time to reach a target strength. In order to adequately investigate this approach, the curing conditions were varied for the Type 1 concrete mixtures in the experiments either through the addition of admixtures or, as in the case of the 030214B batch, by changing the curing temperature (the cylinders were cured in an ice-water bath). These alterations ensured that the target strength was reached at a range of different ages. The strength-velocity relationship used to predict the strength was based on a regression line calculated from the combined set of data from all of the Type 1 mixtures.

A target strength, $f_{c,\,target}$, of 24.1 MPa (3500 psi) was selected since this was the desired transfer strength of the precast plant where testing was performed. It is noted that this strength is within the first linear part of the natural log of strength versus age plot described earlier.

The time to reach the target strength was estimated using three different methods for calculating the regression line. The first was using all data points collected up to a given point in time, the second was using the three most recent points collected up to a given point in time, and the third was using the five most recent points collected up to a given point in time.

6.3.1 Regression Based on All Collected Points

This method for predicting time to reach a target strength uses all of the data points collected up to a given point in time for calculating the regression line. The first calculation of the predicted time to reach the target strength is made after the first two successive data points are taken. When the third data point is taken, the regression line is recalculated using all three points, and the predicted time to reach the target strength is recalculated. This process is repeated when the fourth point, fifth point, and so on are collected until the target strength is actually reached.

6.3.2 Regression Based on Three Most Recent Points

This method uses only the three most recent data points to compute the regression line. This method may be more sensitive to changes in the rate of strength gain of concrete during the time period between the first successful impact-echo test and the time when the target strength is reached. Taking the most recent points into account should allow for any changes to be more quickly detected since the data from the earlier curing rate are not included to bias the prediction. Section 6.4 clearly demonstrates the validity of this approach with the data from the 030214B batch, which was cured in an ice-water bath.

6.3.3 Regression Based on Five Most Recent Points

This method is similar to the previously described method using only the three most recent points. Concerns for possible over-sensitivity to change when using only the three most recent points prompted the exploration of using the five most recent points in time prediction.

6.4 COMPARISON OF REGRESSION METHODS

Figures 6.4 through 6.9 show the results for the six Type 1 mixtures tested with the three different linear regression prediction methods described above. Each of the figures are plots showing the predicted times to reach the target strength using the three linear regression methods. The x-axis ranges down to zero at the right of the plot, which corresponds to the time when the mixture actually reached the target strength. The x-value of each plotted data point therefore represents the amount of time between the prediction and the actual time of the target strength. The y-axis value for each data point represents the time value predicted for when the mixture would reach the target strength. The solid horizontal line is at a y-value corresponding to the actual time the target strength was reached. Figures 6.4 through 6.8 are plotted with a vertical axis range of six hours in order to aid in comparing the vertical scatter from method to method and from batch to batch. This was not possible in Figure 6.9 due to a larger scatter in the vertical axis direction. The horizontal axis ranges in Figures 6.4 through 6.9 are minimized on a case to case basis to avoid masking data points.

A trend that is observed in all of the plots is that in most cases, the methods tend to under-predict the time to reach the target strength. The reasons for this are not known. As the actual time to reach the target strength approaches, the predicted values tend to become more accurate. Also noteworthy are the outlying points that are apparent in some of the figures. During the experiments, it was found that at random, some test cylinders were curing at a different rate than the rest. These differences would cause a noticeable bias to the time prediction values for the methods using only the recent data points, hence the outlying points seen in the figures. However, the effects of these outlying points were negated as additional data points were collected.

With the exception of the 030214B batch, the three methods of calculating a regression line do not appear to have noticeable differences in their accuracy of prediction. The scatter in predicted time values does not clearly show any one method to be more accurate than the others. However, this is not the case for the 030214B batch. The methods which take only the most recent data points into account clearly maintain more accuracy as the target strength is approached. The test cylinders for this batch were kept in an ice-water bath, but after twelve hours from the pour, ice was no longer added, allowing the water temperature to slowly increase. This action caused the situation which was described earlier—the mixture curing rate changed during the testing and the regression method using all points was biased by the earlier data and did not reflect the increase in the rate of strength gain of the concrete as the ice-water bath temperature increased.

6.5 CONCLUSIONS

Examination of the experimental data revealed that the relationship between the natural log of strength and age of a concrete mixture is approximately bi-linear. A general method is proposed to predict the time when a concrete mixture reaches a target compressive strength, $f_{c,\,target}$. The method is applicable only when the natural log of $f_{c,\,target}$ is on the first linear part of the bi-linear relationship between the natural log of strength and velocity.

The three linear regression methods explained work reasonably well. In general, they tend to under-predict the time to reach a target strength, but become more accurate as the actual time of the target strength is approached. The methods utilizing only recently collected data up to a given time show greater sensitivity to changes in the curing rate of a concrete mixture and perhaps over-sensitivity to sudden, short-term changes in the curing rate. Conversely, the method utilizing all collected data points up to a given time shows less tendency to be biased by short-term changes in the curing rate, but an under-sensitivity to long-term changes occurring after a number of data points have been collected.

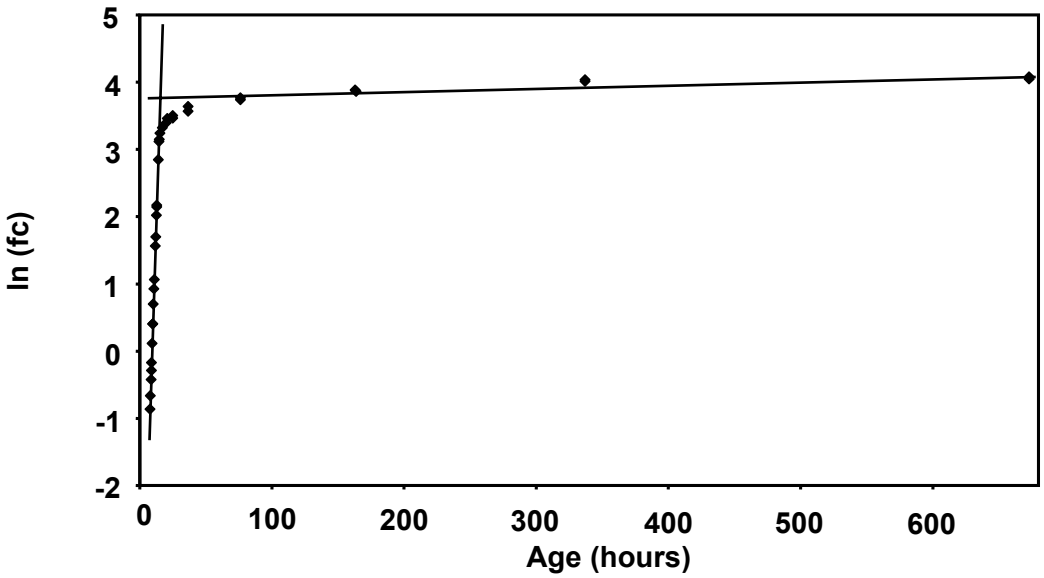

Figure 6.1 – Natural log of strength versus age data through 28 days, for 030214A batch

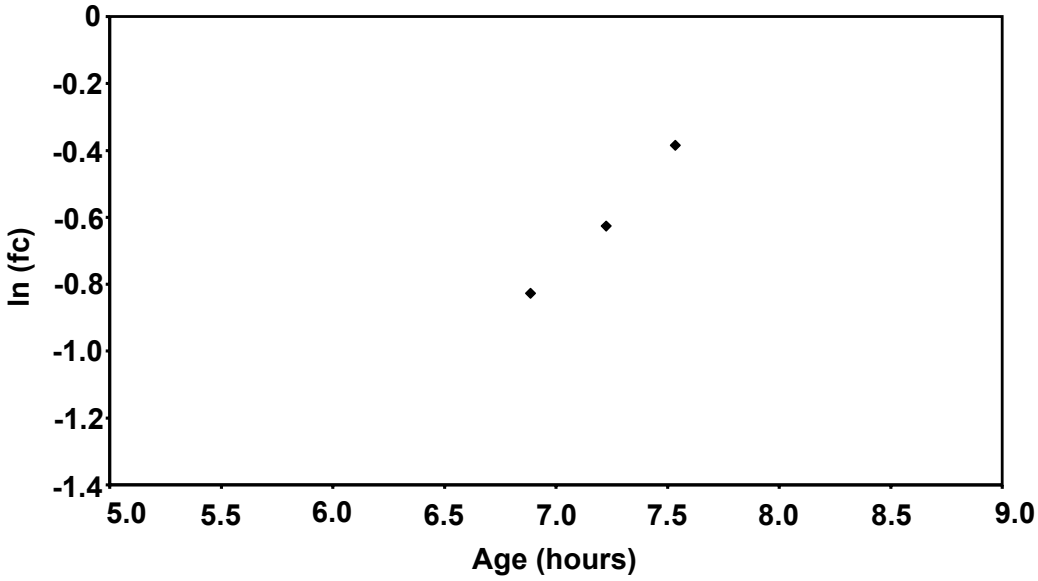

Figure 6.2 – Natural log of strength versus age

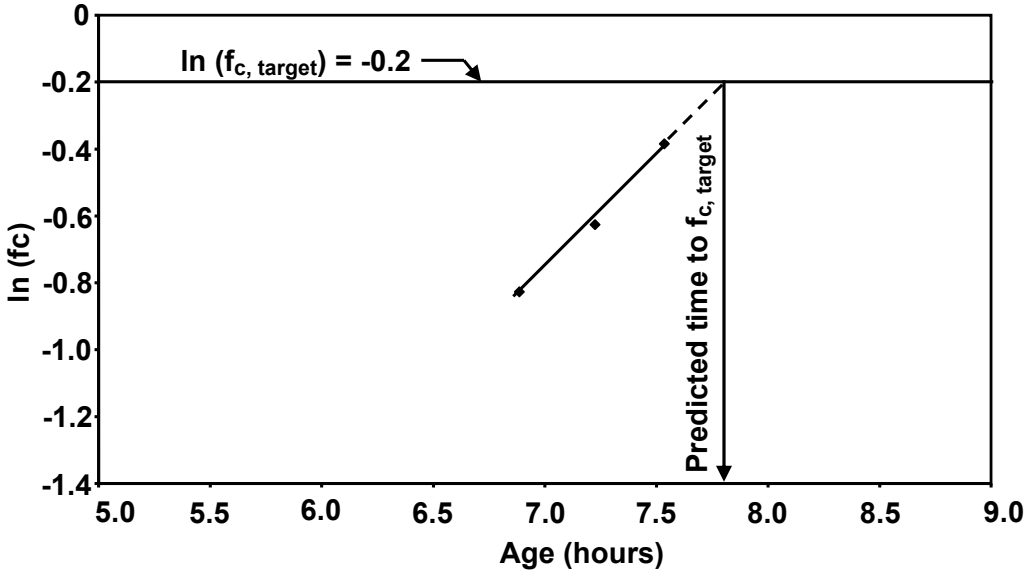

Figure 6.3 – Regression line fitted to natural log of strength versus age

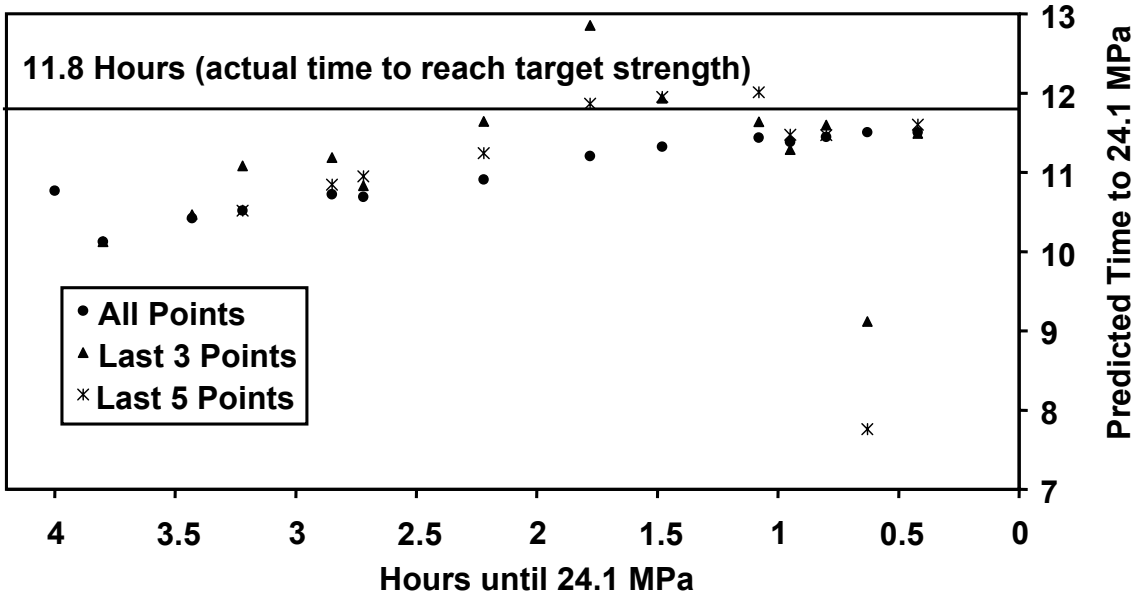

Figure 6.4 – 020808A batch prediction graph

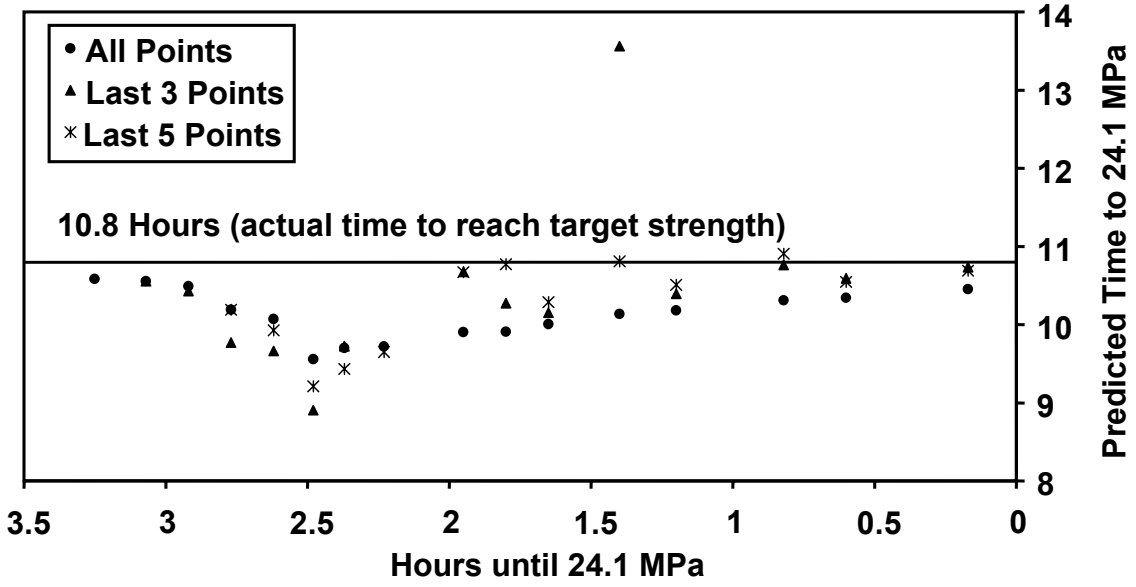

Figure 6.5 – 020812A batch prediction graph

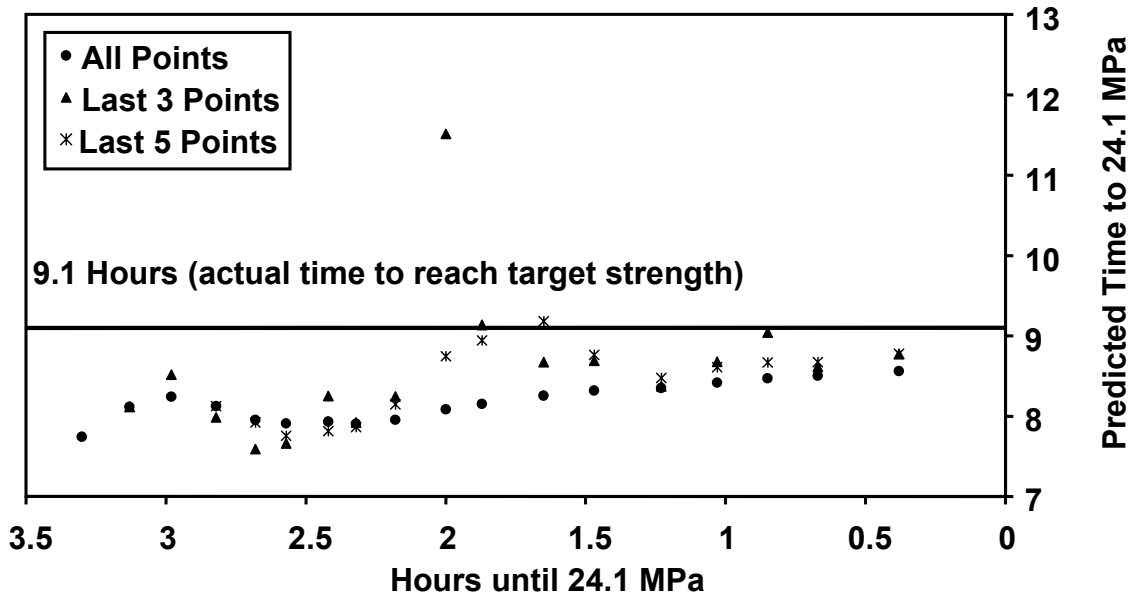

Figure 6.6 – 020812B batch prediction graph

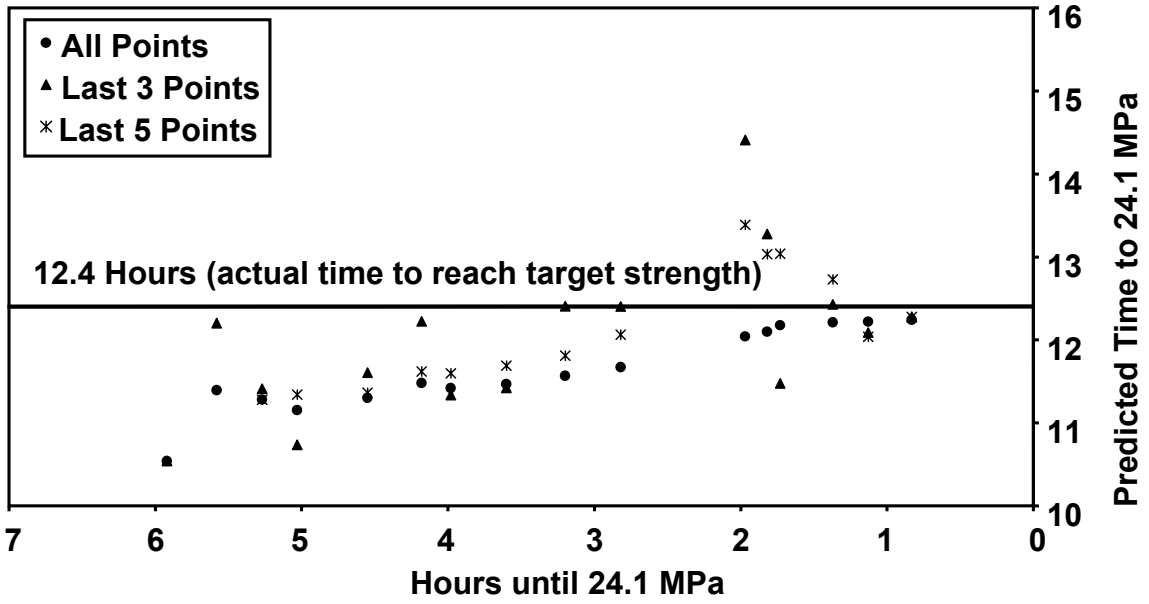

Figure 6.7 – 030108A batch prediction graph

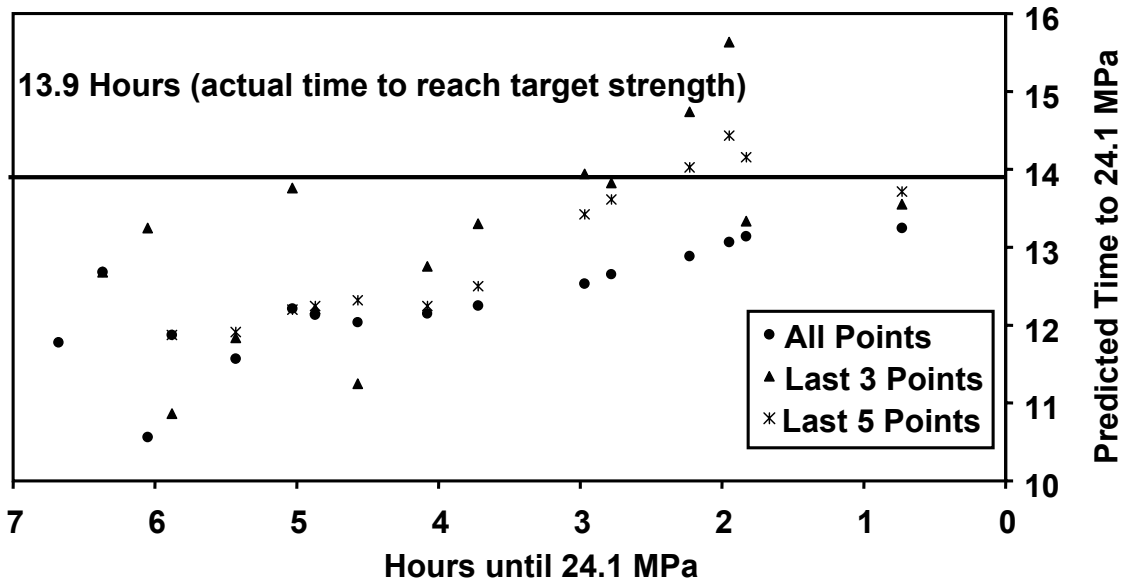

Figure 6.8 – 030214A batch prediction graph

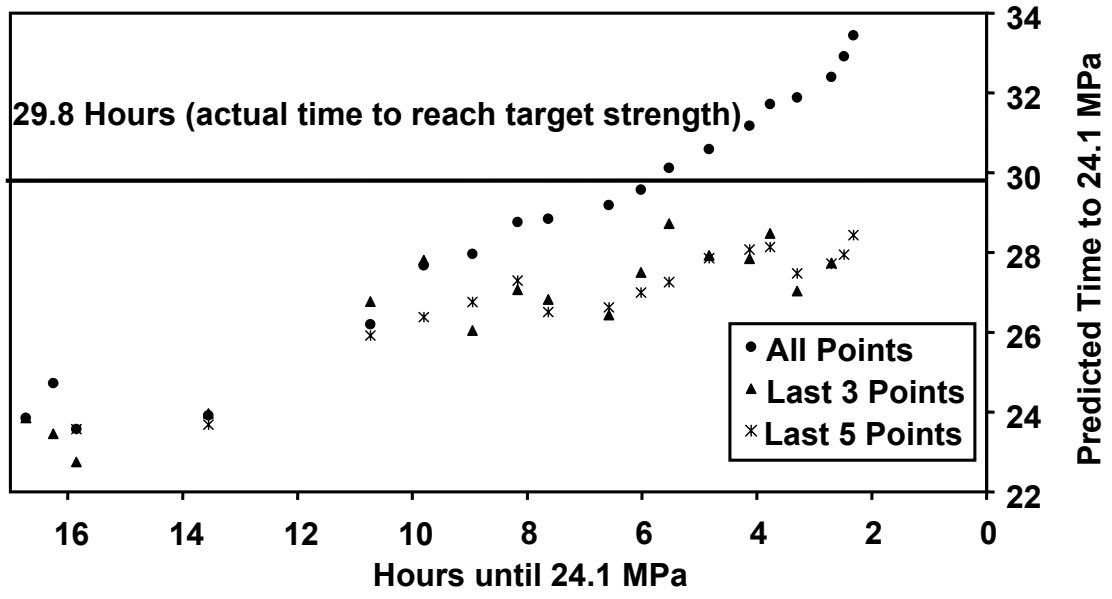

Figure 6.9 – 030214B batch prediction graph

CHAPTER 7

SUMMARY AND CONCLUSIONS

7.1 SUMMARY

Concrete compressive strength is a key parameter used to control the production of precast concrete members. In current practice, concrete compressive strength is often determined by compression tests of cylinders made from the same concrete as the concrete members. The cylinders are cured in a manner that is intended to replicate the curing conditions in the actual concrete members.

The objectives of this research were to explore the ability of the impact-echo method to be used as a tool for quality control, and to determine if the impact-echo method can be used to evaluate the rate of strength gain of a concrete mixture.

Tests were performed on seven batches of concrete cylinders in a precast plant. Six of the seven batches of cylinders were made with the same concrete mixture, and the other batch utilized a different concrete mixture. The cylinders were 152mm diameter by 305mm high (6 inch x 12 inch) in size and were prepared in accordance with ASTM standards. The impact-echo method was used to measure the P-wave velocity and this data was recorded along with the time of the test. Immediately following the impact-echo test, the cylinder was tested in compression and the compressive strength was recorded. This procedure was repeated many times in order to gather an adequate amount of data to meet the research goals.

7.2 CONCLUSIONS

7.2.1 Using the Impact-Echo Method to Estimate Strength

Chapter 2 discussed previous research regarding the use of the impact-echo method to estimate the strength of a concrete mixture. Chapter 4 explained how this ability is a valuable tool for a precast plant. Concrete cylinders do not have to be tested in compression until impact-echo tests show that the target strength has been reached. This can eliminate the risk of running out of cylinders in the event that a concrete mixture is not curing at the rate that it is intended to.

7.2.2 Use of the Impact-Echo Method for Quality Control

Previous research, discussed in Chapter 2, has shown that variations in the ingredient portions of a concrete mixture can influence the relationship between compressive strength and P-wave velocity.

Confidence limits were calculated for the mean of the natural log of strength versus P-wave velocity data from several experiments utilizing the same concrete mixture. When data from a concrete mixture with differing ingredients was superimposed on these confidence limits, it crossed outside of the confidence limits. Therefore, confidence limits can be used in combination with the impact-echo method to monitor deviations in the ingredients of a concrete mixture.

Confidence limits should be calculated for the strength-velocity curve used to predict strength. Periodic testing should be performed to ensure that the natural log of strength versus P-wave velocity data stays within these limits, and if not, a new strength-velocity relationship should be developed in order to maintain accurate strength prediction.

7.2.3 Use of the Impact-Echo Method to Predict Time to Reach a Target Strength

Examination of the experimental data revealed that the relationship between the natural log of strength and age of a concrete mixture is approximately bi-linear. A general method is proposed to predict the time when a concrete mixture reaches a target compressive strength, $f_{c,\ target}$. The method is applicable only when the natural log of $f_{c,\ target}$ is on the first linear part of the bi-linear relationship between the natural log of strength and velocity.

The three linear regression methods explained work reasonably well. In general, they tend to under-predict the time to reach a target strength, but become more accurate as the actual time of the target strength is approached. The methods utilizing only recently collected data up to a given time show greater sensitivity to changes in the curing rate of a concrete mixture and perhaps over-sensitivity to sudden, short-term changes in the curing rate. Conversely, the method utilizing all collected data points up to a given time shows less tendency to be biased by short-term changes in the curing rate, but an under-sensitivity to long-term changes occurring after a number of data points have been collected.

REFERENCES

Montgomery, D., Runger, G., Applied Statistics and Probability for Engineers, John Wiley & Sons, 1994, 895 pp.

Pessiki, S., Carino, N., "Setting Time and Strength of Concrete Using the Impact-Echo Method," *Materials Journal*, ACI, Vol. 85, No. 5, September-October 1988, pp. 389-399.

Pessiki, S., Johnson, M., "Nondestructive Evaluation of Early-Age Concrete Strength in Plate Structures by the Impact-Echo Method," *Materials Journal*, ACI, Vol. 93, No. 3, May-June 1996, pp. 260-271.

Pessiki, S., Rowe, M., "Influence of Steel Reinforcing Bars on the Evaluation of Early-Age Concrete Strength Using the Impact-Echo Method," *Structural Journal*, ACI, Vol. 94, No. 4, July-August 1997, pp. 378-388.

Sansalone, M., Streett, W., Impact-Echo: Nondestructive Evaluation of Concrete and Masonry, Bullbrier Press, 1997, 339 pp.

APPENDIX A

DATA FROM CONCRETE MIXTURES

020808A batch		
Age (hours)	Velocity (km/s)	fc (MPa)
7.43	1.22	0.34
7.80	1.52	0.63
8.00	1.81	0.93
8.37	2.04	1.17
8.58	2.21	1.61
8.95	2.43	2.54
9.08	2.61	2.78
9.58	2.80	4.73
10.02	2.93	5.85
10.32	3.16	8.34
10.72	3.35	10.39
10.85	3.64	16.73
11.00	3.51	12.29
11.17	3.58	16.29
11.38	3.83	22.04
11.52	3.77	20.92
11.62	3.71	21.80
12.00	3.91	27.68
12.28	3.94	26.95
12.67	4.02	29.51
13.00	4.01	30.60
14.00	4.09	33.90
16.00	4.18	37.19
20.00	4.15	40.11
20.17	4.21	40.36
24.00	4.21	42.92
24.00	4.19	41.82
36.00	4.22	42.80
36.00	4.30	42.74
72.00	4.34	45.97
72.00	4.36	45.97
168.00	4.38	51.21
168.00	4.39	50.36
336.00	4.42	56.57
336.00	4.37	55.54
672.00	4.47	59.62
672.00	4.49	61.69

020812A batch		
Age (hours)	Velocity (km/s)	fc (MPa)
7.33	1.27	0.39
7.55	1.44	0.49
7.73	1.59	0.68
7.88	1.73	0.78
8.03	1.94	0.93
8.18	2.09	1.41
8.32	2.61	3.17
8.43	2.34	1.76
8.57	2.58	2.58
8.85	2.65	3.56
9.00	2.96	5.41
9.15	2.93	4.68
9.40	3.04	6.44
9.60	3.30	7.46
9.98	3.41	9.46
10.20	3.71	14.88
10.63	3.81	20.43
10.97	3.92	25.73
11.23	3.99	27.56
11.62	4.02	27.19
12.00	4.01	29.75
12.33	4.06	31.34
12.77	4.02	31.70
13.28	4.06	31.46
13.90	4.14	32.80
16.00	4.18	35.48
20.00	4.24	38.77
24.00	4.21	39.87
24.00	4.27	38.65
36.00	4.27	41.21
36.00	4.19	40.24
72.00	4.38	43.89
72.00	4.30	42.92
168.00	4.38	46.70
168.00	4.41	47.73
336.00	4.39	52.43
336.00	4.37	50.72
672.00	4.47	56.45
672.00	4.41	56.82

020812B batch		
Age (hours)	Velocity (km/s)	fc (MPa)
5.63	1.23	0.29
5.80	1.44	0.49
5.97	1.59	0.68
6.12	1.73	0.63
6.28	1.95	1.02
6.42	2.18	1.37
6.53	2.30	1.51
6.68	2.43	2.19
6.78	2.60	2.73
6.92	2.66	2.88
7.10	2.69	2.73
7.23	2.84	3.95
7.45	2.96	4.54
7.63	3.14	6.00
7.87	3.39	9.66
8.07	3.45	8.88
8.25	3.57	11.22
8.43	3.76	17.41
8.72	3.86	20.48
9.22	3.96	25.60
9.48	4.02	26.58
9.87	3.99	28.77
10.25	4.02	29.26
10.63	4.07	30.73
11.33	4.11	31.09
12.00	4.14	31.70
14.00	4.19	34.63
16.00	4.22	37.19
20.00	4.24	39.63
24.00	4.28	39.38
24.00	4.30	39.87
36.00	4.27	39.99
36.00	4.28	40.42
72.00	4.33	42.25
72.00	4.33	43.65
168.00	4.39	47.25
168.00	4.40	46.94
336.00	4.43	50.36
336.00	4.40	49.99
672.00	4.47	55.35
672.00	4.47	56.45

030108A batch		
Age (hours)	Velocity (km/s)	fc (MPa)
6.15	1.15	0.34
6.23	1.27	0.39
6.48	1.38	0.44
6.82	1.53	0.59
7.13	1.71	0.63
7.37	1.86	0.73
7.85	2.07	1.07
8.22	2.22	1.22
8.42	2.38	1.85
8.80	2.53	2.10
9.20	2.68	2.88
9.58	2.83	4.05
10.43	2.98	5.95
10.58	3.19	9.85
10.67	3.17	8.63
11.03	3.35	13.80
11.27	3.48	16.58
11.57	3.59	19.75
11.73	3.63	20.73
12.00	3.69	23.04
12.00	3.68	22.31
12.53	3.75	25.00
13.63	3.86	27.80
15.02	3.87	30.12
15.95	3.92	31.70
16.03	3.96	31.46
17.85	4.03	33.29
17.90	4.01	32.55
24.00	4.08	36.58
24.00	4.06	36.09
36.80	4.14	39.63
36.98	4.12	40.11
72.38	4.24	43.22
72.67	4.23	44.99
175.62	4.35	51.70
175.72	4.32	50.72
346.32	4.35	54.87
346.40	4.35	55.23
671.15	4.42	61.52
671.32	4.41	57.92
671.48	4.47	59.72
671.73	4.44	61.38

030108B batch		
Age (hours)	Velocity (km/s)	fc (MPa)
6.87	1.16	0.39
7.05	1.30	0.39
7.48	1.49	0.66
7.68	1.67	0.78
7.82	1.89	0.88
8.53	2.03	1.32
8.73	2.16	1.71
9.10	2.35	2.07
9.63	2.53	3.41
10.22	2.68	4.93
10.65	2.90	6.68
10.95	3.04	7.46
11.22	3.19	10.12
12.02	3.44	15.00
12.05	3.44	16.34
12.53	3.54	17.92
13.05	3.56	20.36
14.08	3.69	22.68
14.13	3.65	23.53
15.97	3.81	25.97
16.02	3.83	27.92
20.52	3.98	31.70
24.52	4.01	35.97
24.70	4.05	37.80
35.90	4.11	41.33
36.05	4.06	41.03
71.48	4.21	52.31
71.72	4.21	51.03
173.45	4.44	65.96
173.77	4.36	63.16
333.07	4.38	67.11
333.23	4.35	65.45
668.15	4.39	68.74
668.48	4.36	67.40
668.68	4.41	70.08
668.88	4.35	67.25

030214A batch		
Age (hours)	Velocity (km/s)	fc (MPa)
6.88	1.23	0.44
7.22	1.41	0.54
7.53	1.53	0.68
7.85	1.68	0.78
8.02	1.90	0.88
8.47	2.05	1.17
8.87	2.20	1.56
9.03	2.35	1.56
9.33	2.53	2.10
9.82	2.68	2.63
10.18	2.83	3.02
10.93	3.02	4.97
11.12	3.13	5.71
11.67	3.20	7.85
11.95	3.28	8.93
12.07	3.39	9.17
13.17	3.76	18.00
13.58	3.95	23.53
14.00	3.95	24.26
14.55	3.98	26.58
16.20	4.09	28.90
19.00	4.17	31.21
19.93	4.17	33.16
23.93	4.09	33.41
24.10	4.17	34.63
35.75	4.30	39.57
35.80	4.14	36.88
75.17	4.24	43.95
75.30	4.29	45.11
162.97	4.38	49.75
162.10	4.33	50.66
336.00	4.45	57.67
336.00	4.49	58.89
672.00	4.49	61.69
672.00	4.49	59.56

030214B batch		
Age (hours)	Velocity (km/s)	fc (MPa)
11.25	1.12	0.24
12.22	1.27	0.29
13.07	1.53	0.44
13.55	1.56	0.49
13.95	1.75	0.63
16.25	2.20	1.27
19.07	2.61	2.39
20.00	2.75	3.32
20.85	2.94	4.54
21.63	3.02	5.90
22.17	3.16	6.00
23.22	3.31	9.12
23.78	3.39	11.12
24.27	3.42	11.80
24.97	3.54	13.31
25.67	3.61	15.66
26.03	3.65	17.61
26.50	3.80	19.02
27.10	3.80	20.36
27.32	3.80	21.95
27.48	3.80	20.73
28.00	3.80	21.70
36.00	4.14	32.68
75.40	4.27	44.02
672.00	4.52	65.66
672.00	4.52	64.68